Supplementary Figures

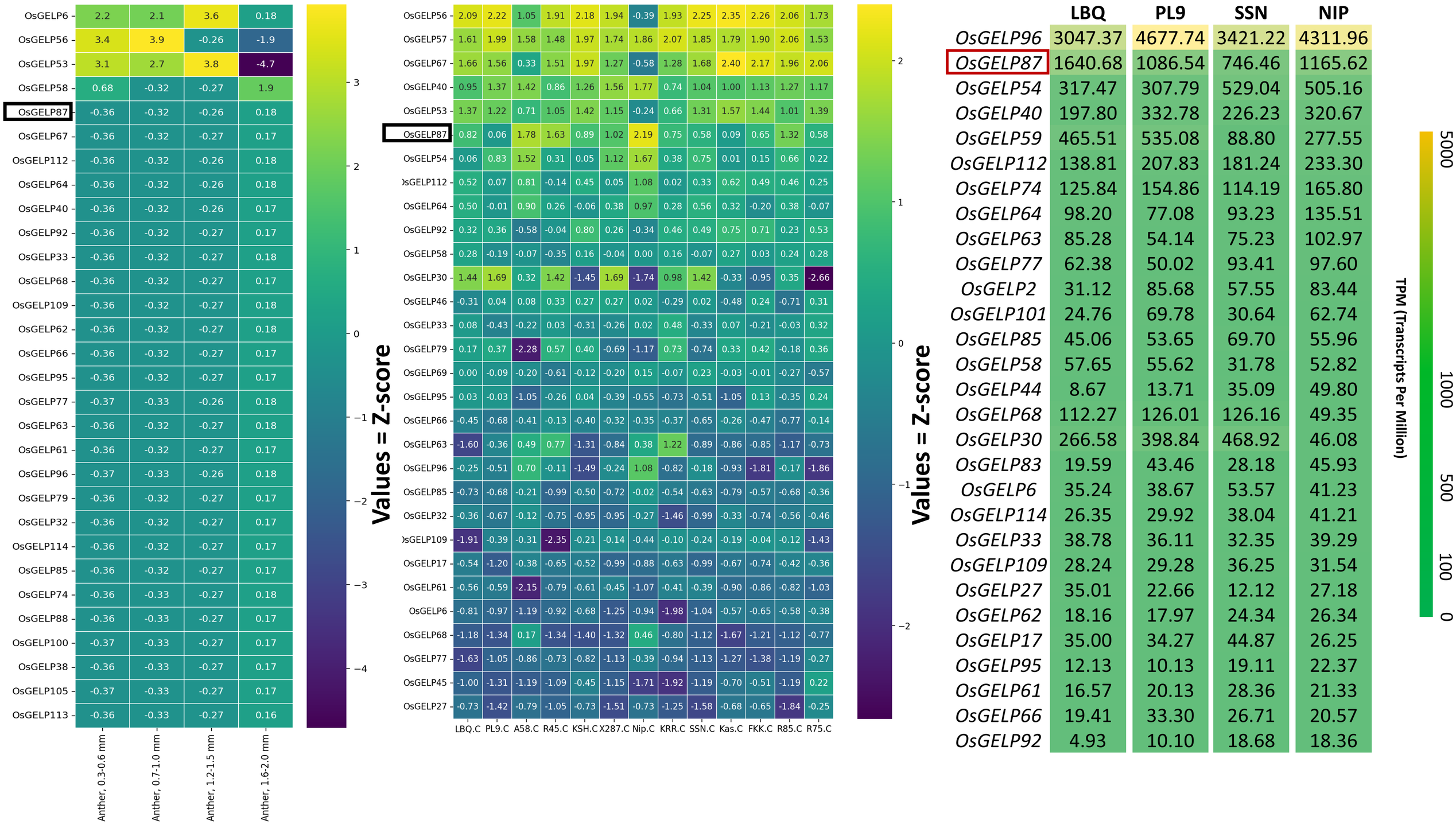

Fig. S1 OsGELPs gene expression level (a) Normalized relative expression in *OsGELP* genes based on RiceXPro database in anther organ. The expression data were not available in *OsGELP13, OsGELP28, OsGELP34, OsGELP36, OsGELP39, OsGELP41, OsGELP48, OsGELP57, OsGELP60, OsGELP104*, and *OsGELP115*. Expression levels of OsGELP genes from RiceXPro were converted to z-scores. The genes were sorted in order of highest average z-score in four stages. There are 104 OsGELP genes with expression levels. The heatmap was shown for the 30 genes with the highest z-score. OsGELP87 indicates 5th highest expression level. **(b) Microarray data was extracted from Yamamori et al., 2024 and converted into z-score.** The genes were sorted in order of highest average z-score in booting stages. The heatmap was drawn for the 30 genes with the highest z-score. The x axis shown the rice varieties (LBQ: Lambeqyue; PL9: Hokkai PL9; KSH: Koshihikari; K287: Kirara287; NIP: Nipponbare; SSN: Sasanishiki; Kas: Kasalat; FKK: Fukoku). **(c) Expression profiles of OsGELP genes in rice anthers at the booting stage.** RNA-seq data were extracted from Yamamori et al. (2024). The 30 OsGELP genes with the highest transcript abundance (TPM: Transcripts Per Million) were selected and ranked in descending order of expression. Heatmap values represent TPM levels across four rice varieties: Lambequye (LBQ), Hokkai PL9 (PL9), Sasanishiki (SSN), and Nipponbare (NIP). Expression intensities are color-coded from low (green) to high (yellow).

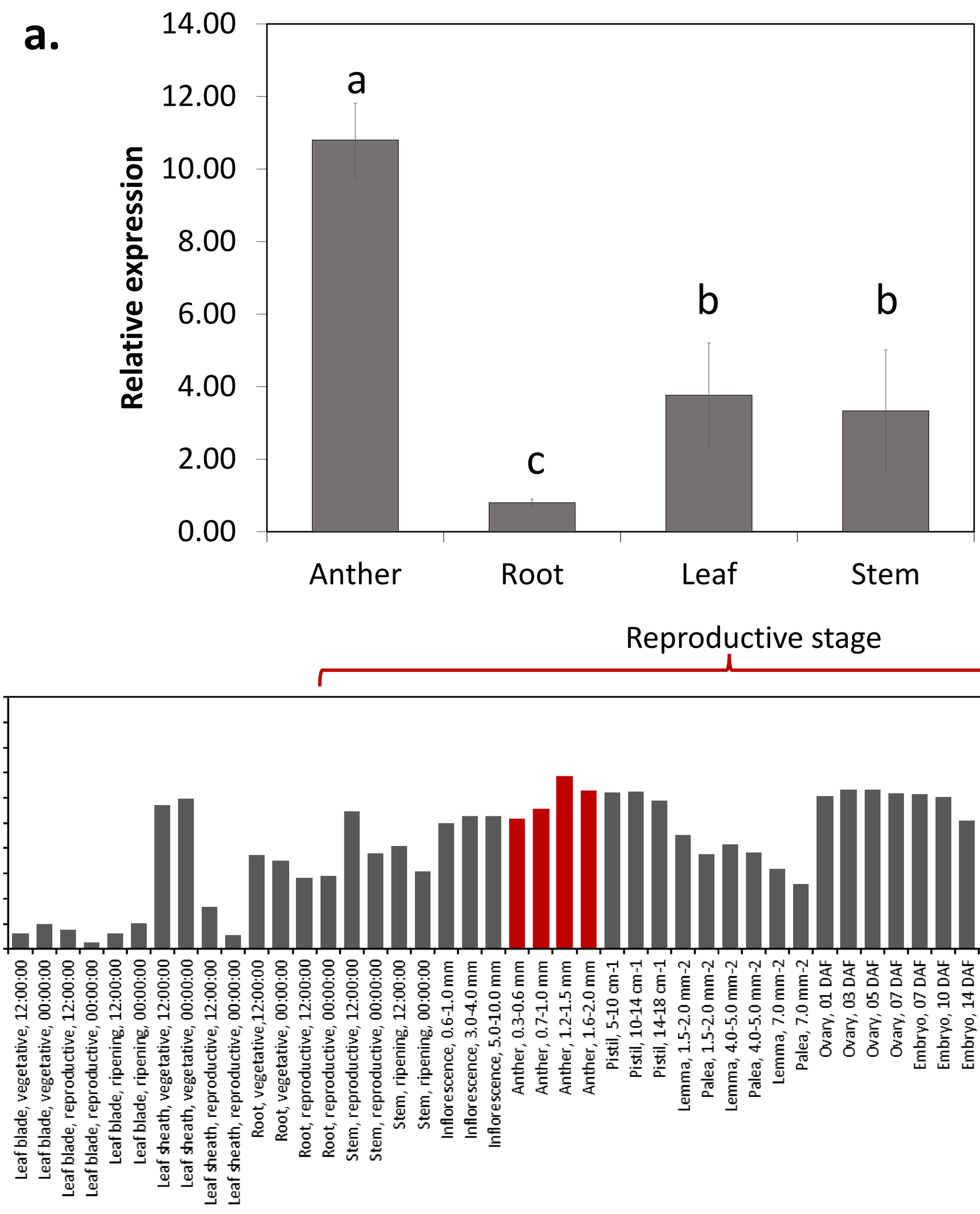

Fig. S2 Tissue-specific expression of *OsGELP87* determined by qRT-PCR.

(a) Quantitative real-time PCR analysis showing the relative expression levels of *OsGELP87* in rice anther, shoot, root, leaf, and stem. Transcript abundance was normalized to an internal reference gene and calculated using the $2^{-}\Delta\Delta Ct$ method. Data represent the mean ± SD of three biological replicates. *OsGELP87* exhibits markedly higher expression in anthers compared with vegetative tissues, indicating anther-preferential expression and suggesting a specialized role in reproductive development. **(b) Expression Profiles of GELP Gene Family Members in Various Rice Tissues.** Expression levels of OsGELP87 was analyzed across multiple rice tissues and developmental stages were obtained from the RiceXPro database and are presented as log2-transformed values. The y-axis represents normalized log2 expression levels, while the x-axis lists specific rice tissues or developmental stages. Bars highlighted in **red** indicate significant expression peaks in reproductive tissues, such as anthers or pollen.

a.

ID	Position	Peptide	Score	Cutoff	Type
OsGELP87	267	LNALRGGCVEEYNQV	2,419	2,293	S-Palmitoylation: Cluster B
OsGELP87	376	ANSTLQICLRELLS*	3,129	1,079	S-Palmitoylation: Cluster A

b.

Genes	WoLF PSORT	Plant-mPLoc	DeepLoc 2.0
OsGELP87	extr: 9, golg: 2, chlo: 1, mito: 1	Extracellular	Extracellular

c.

OsGELP87
Prediction: Signal Peptide (Sec/SPI)

Cleavage site between pos. 30 and 31.
Probability 0.959843

Protein type	Other	Signal Peptide (Sec/SPI)	Lipoprotein signal peptide (Sec/SPII)	TAT signal peptide (Tat/SPI)	TAT Lipoprotein signal peptide (Tat/SPII)	Pilin-like signal peptide (Sec/SPIII)
Likelihood	0.0039	0.9949	0.0005	0.0003	0.0002	0.0002

Download: PNG / EPS / Tabular

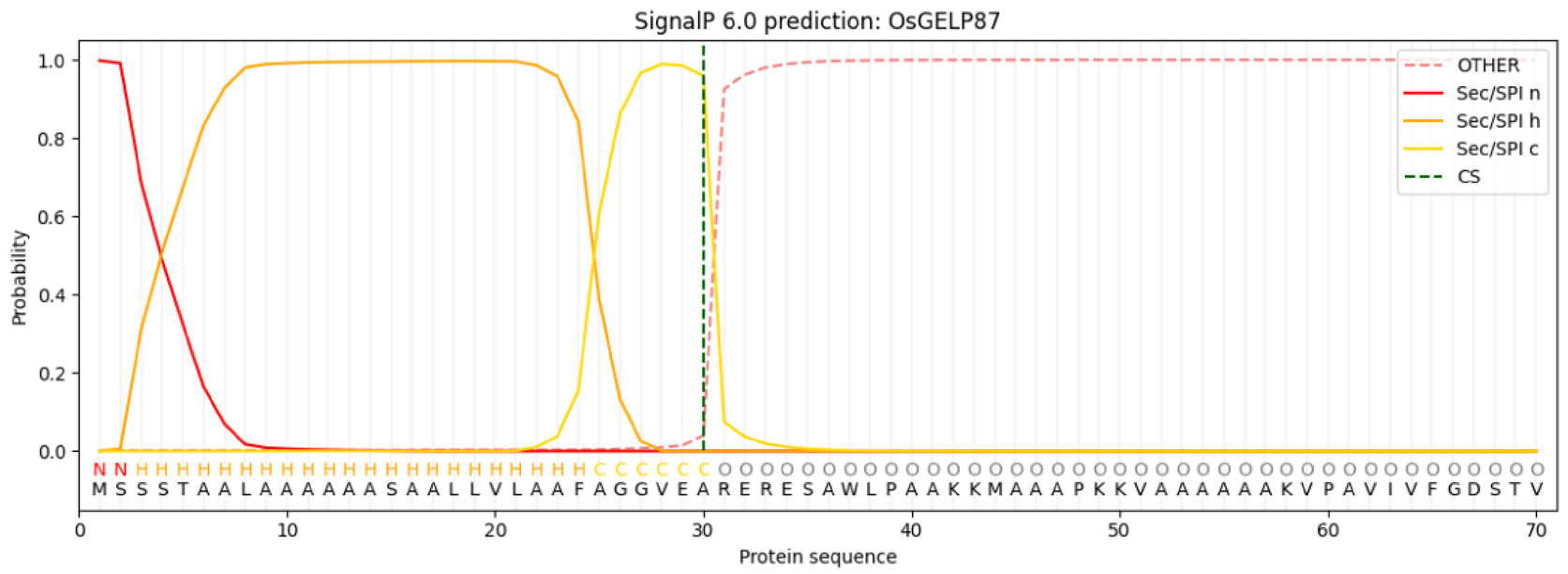

Fig. S3 In silico prediction of lipid modification sites and subcellular localization of OsGELP87. (a) Prediction of lipid modification sites using GPS-Lipid identified two putative **S-palmitoylation sites** at Cys267 and Cys376, both above the medium cutoff threshold, belonging to cluster B and cluster A, respectively. **(b)** Subcellular localization analysis using WoLF PSORT, Plant-mPLoc, and DeepLoc predicted OsGELP87 to be targeted mainly to the **extracellular space** or secretory pathway, with additional possible signals for Golgi, chloroplast, and mitochondria. **(C)** Signal peptide analysis with SignalP 6.0 revealed a strong **N-terminal signal peptide cleavage site** between positions 30 and 31, with high prediction probability (0.959843), supporting secretion or membrane-associated localization.

a.

```
OsGELP32    MA----------SPLVRLLLLLLVV---------------AAASRGAASAAKAKAARVT 35
OsGELP87    MSSSTAALAAAAAASAALLVLAAFAGGVEARERESAWLPAAKKMAAAPKKVAAAAAAKVP 60

OsGELP32    AVIVFGDSTVDTGNNNQIGTPLRSDFPPYGRDMPGGARATGRFGNGRLAPDFMSESLGLP 95
OsGELP87    AVIVFGDSTVDTGNNNVVATMLKSNFPPYGRDLG---AATGRFCNGRLPPDFMSEALGLP 117

OsGELP32    PLVPAYLDPAYGIADFARGVCFASAGTGLDNATAGVLSVIPLWKEVEYYREYQRRLRAHA 155
OsGELP87    PLVPAYLDPAYGIADFARGVCFASAGTGLDNATAGVLAVIPLWKEVEYFKEYQRRLRRHA 177

OsGELP32    GAAAARDVVRGALHVVSIGTNDFLENYYMLATGRFARYSVGEYEDYLVAAARAFLAAIHR 215
OsGELP87    GRAAARRIVRDALYVVSIGTNDFLENYFLLVTGRFKQFTVGEFEDFLVAQAAGFLAAIHR 237

OsGELP32    LGARRVTFAGLSPMGCLPLERTAGALLGGGGGGCVEEYNRVAREYNGKVEAMVRSLRAEL 275
OsGELP87    LGARRVAFAGLSAIGCLPLERTLNAL----RGGCVEEYNQVARDYNVKLNAMIAGLQSSL 293

OsGELP32    PRLKVAFIPVYDNMLDLITHPEKYGLENVEEGCCATGRFEMGFMCNDESPLTCDDASKYL 335
OsGELP87    PGLKIAYVPVYDDMLNLINNPSTLGLENVEQGCCATGMFEMSYLCNEKNPLTCPDADKYF 353

OsGELP32    FWDAFHPTEKVNRIMAQHTLDVCYQQGVL364
OsGELP87    FWDSFHPTEKVNRFFANSTLQICLRELLS382
```

b.

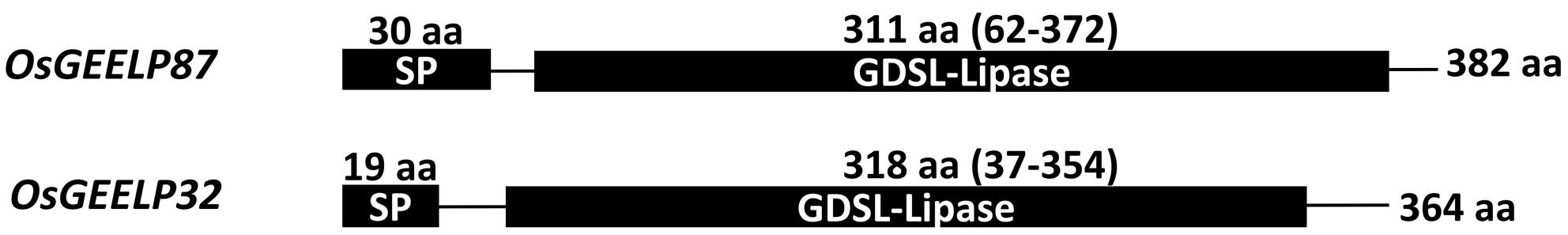

c.

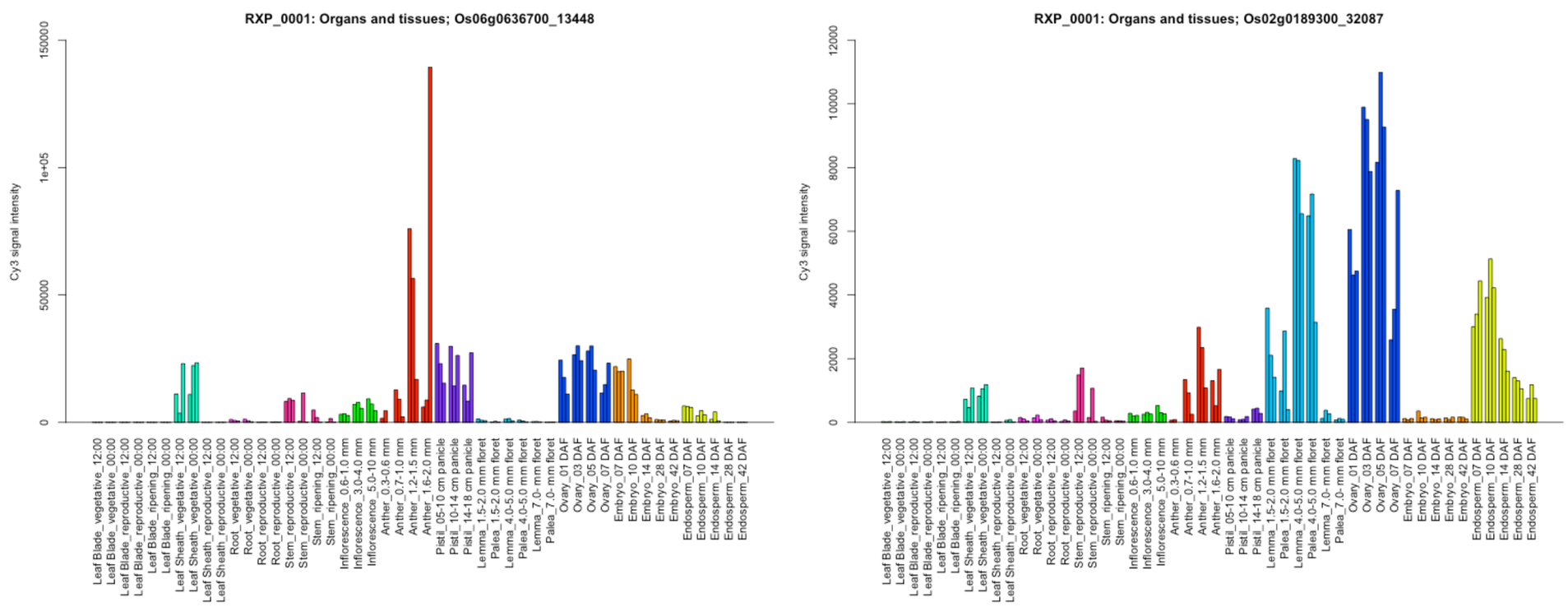

Fig. S4 Sequence alignment and expression profiles of rice GDSL lipase genes OsGELP32 and OsGELP87. (a) Multiple amino acid sequence alignment of OsGELP32 and OsGELP87. Identical or highly conserved residues are highlighted. **(b)** Both proteins contain an N-terminal signal peptide (SP) followed by the conserved GDSL lipase/esterase domain, including the characteristic catalytic motifs of the GDSL family, indicating shared enzymatic features despite sequence divergence. **(c)** Expression profiles of **OsGELP32** (left) and **OsGELP87** (right) across rice organs and developmental stages based on public transcriptomic datasets. OsGELP32 shows broader expression with moderate levels in multiple tissues, whereas OsGELP87 displays strong enrichment in reproductive organs, particularly anthers and panicles, suggesting functional specialization following gene duplication.

a.

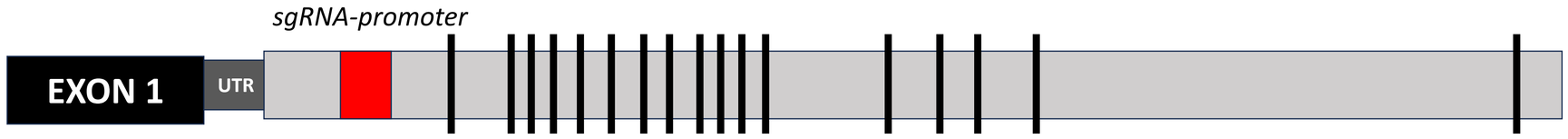

Subpopulation Group	Haplotype	Promoter (2000 bp) (6:25876285-25878285)																	
		1	2	3	4	5	6	7	8	9	10	11	12	13	14	15	16	17	18
Sub. I	Hap.2	G	T	A	A	G	A	G	T	T	T	A	T	T	T	C	C	A	G
Sub. J	Hap.1	A	C	T	G	A	G	T	C	C	C	G	C	A	C	T	C	G	A
	Hap.4	A	C	T	G	A	G	T	C	C	C	G	C	A	C	T	C	G	A
	Hap.5	A	C	T	G	A	G	T	C	C	C	G	C	T	C	T	T	G	A

b.

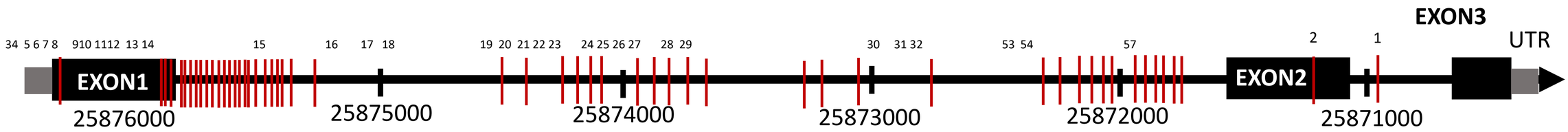

Chr.pos.	IRGSP-1.0	1	2	3	4	5	6	7	8	9	10	11	12	13	14	15	16	17	18	19	20	21	22	23	24	25	26	27	28	29	30	31	32	33	34	35	36	37	38	39	40	41	42	43	44	45	46	47	48	49	50	51	52	53	54	55	56	57	Hap.	Pollen Fertility (%)
		25870388	25871246	25871577	25871650	25871840	25871881	25871883	25871940	25872129	25872269	25872274	25872348	25872389	25872421	25872763	25873047	25873369	25873468	25873707	25873736	25873769	25873825	25873865	25874246	25874273	25874441	25874499	25874669	25874683	25875292	25875334	25875338	25875370	25875424	25875431	25875468	25875472	25875505	25875520	25875537	25875543	25875602	25875650	25875663	25875696	25875710	25875717	25875719	25875728	25875740	25875746	25875761	25875804	25876118	25876183	25876184	25876328		
A58		T	C	A	G	A	T	C	G	A	G	G	C	C	C	G	T	G	A	T	A	G	T	A	A	A	C	A	A	T	C	G	G	G	A	T	A	T	A	A	T	G	C	C	C	C	C	T	T	C	C	G	T	A	T	A	C	C	Hap.5	90.61 (a)
NIP (WT)		T	C	A	G	A	T	C	G	A	G	G	C	C	C	G	T	G	A	T	A	G	T	G	T	A	C	A	A	T	C	G	G	G	G	T	A	T	A	A	T	G	C	C	T	C	C	T	T	C	C	G	T	G	G	C	T	T	Hap.4	80.49 (c)
Supa		G	C	T	A	G	A	T	A	C	A	A	T	T	T	T	A	A	C	A	G	A	C	G	A	G	T	G	G	C	T	A	A	A	G	C	G	C	G	A	C	A	C	T	C	T	T	C	C	T	G	C	G	A	G	C	T	T	Hap.2	63.59 (e)
Nene		G	C	T	A	G	A	T	A	C	A	A	T	T	T	T	A	A	C	A	G	A	C	G	A	G	T	G	G	C	T	A	A	A	G	C	G	C	G	A	C	A	C	T	C	T	T	C	C	T	G	C	G	A	G	C	T	T	Hap.2	76.98 (c)
Kasalat		G	C	T	A	G	A	T	A	C	A	A	T	T	T	T	A	A	C	A	G	A	C	G	A	G	T	G	G	C	T	A	A	A	G	C	G	C	G	A	C	A	C	T	C	T	T	C	C	T	G	C	G	A	G	C	T	T	Hap.2	75.92 (c)
I33		G	C	T	A	G	A	T	A	C	A	A	T	T	T	T	A	A	C	A	G	A	C	G	A	G	T	G	G	C	T	A	A	A	G	C	G	C	G	A	C	A	C	T	C	T	T	C	C	T	G	C	G	A	G	C	T	T	Hap.2	78.77 (c)
Kirara		T	A	A	G	A	T	C	G	A	G	G	C	C	C	G	T	G	A	T	A	G	T	G	T	A	C	A	A	T	C	G	G	G	G	T	A	T	A	A	T	G	C	C	T	C	C	T	T	C	C	G	T	G	G	C	T	T	Hap.1	83.78 (b)
PL9		T	A	A	G	A	T	C	G	A	G	G	C	C	C	G	T	G	A	T	A	G	T	G	T	A	C	A	A	T	C	G	G	G	G	T	A	T	A	A	T	G	C	C	T	C	C	T	T	C	C	G	T	G	G	C	T	T	Hap.1	83.50 (b)
Koshihikari		T	A	A	G	A	T	C	G	A	G	G	C	C	C	G	T	G	A	T	A	G	T	G	T	A	C	A	A	T	C	G	G	G	G	T	A	T	A	A	T	G	C	C	T	C	C	T	T	C	C	G	T	G	G	C	T	T	Hap.1	83.47 (b)
T65		T	A	A	G	A	T	C	G	A	G	G	C	C	C	G	T	G	A	T	A	G	T	G	T	A	C	A	A	T	C	G	G	G	G	T	A	T	A	A	T	G	C	C	T	C	C	T	T	C	C	G	T	G	G	C	T	T	Hap.1	93.98 (a)
Kitaake		T	A	A	G	A	T	C	G	A	G	G	C	C	C	G	T	G	A	T	A	G	T	G	T	A	C	A	A	T	C	G	G	G	G	T	A	T	A	A	T	G	C	C	T	C	C	T	T	C	C	G	T	G	G	C	T	T	Hap.1	87.60 (b)
Kitakaori		T	A	A	G	A	T	C	G	A	G	G	C	C	C	G	T	G	A	T	A	G	T	G	T	A	C	A	A	T	C	G	G	G	G	T	A	T	A	A	T	G	C	C	T	C	C	T	T	C	C	G	T	G	G	C	T	T	Hap.1	85.30 (b)
Lambyque1		T	A	A	G	A	T	C	G	A	G	G	C	C	C	G	T	G	A	T	A	G	T	G	T	A	C	A	A	T	C	G	G	G	G	T	A	T	A	A	T	G	C	C	T	C	C	T	T	C	C	G	T	G	G	C	T	T	Hap.1	90.17 (a)
Silewah		T	A	A	G	A	T	C	G	A	G	G	C	C	C	G	T	G	A	T	A	G	T	G	T	A	C	A	A	T	C	G	G	G	G	T	A	T	A	A	T	G	C	C	T	C	C	T	T	C	C	G	T	G	G	C	T	T	Hap.1	92.62 (a)

c.

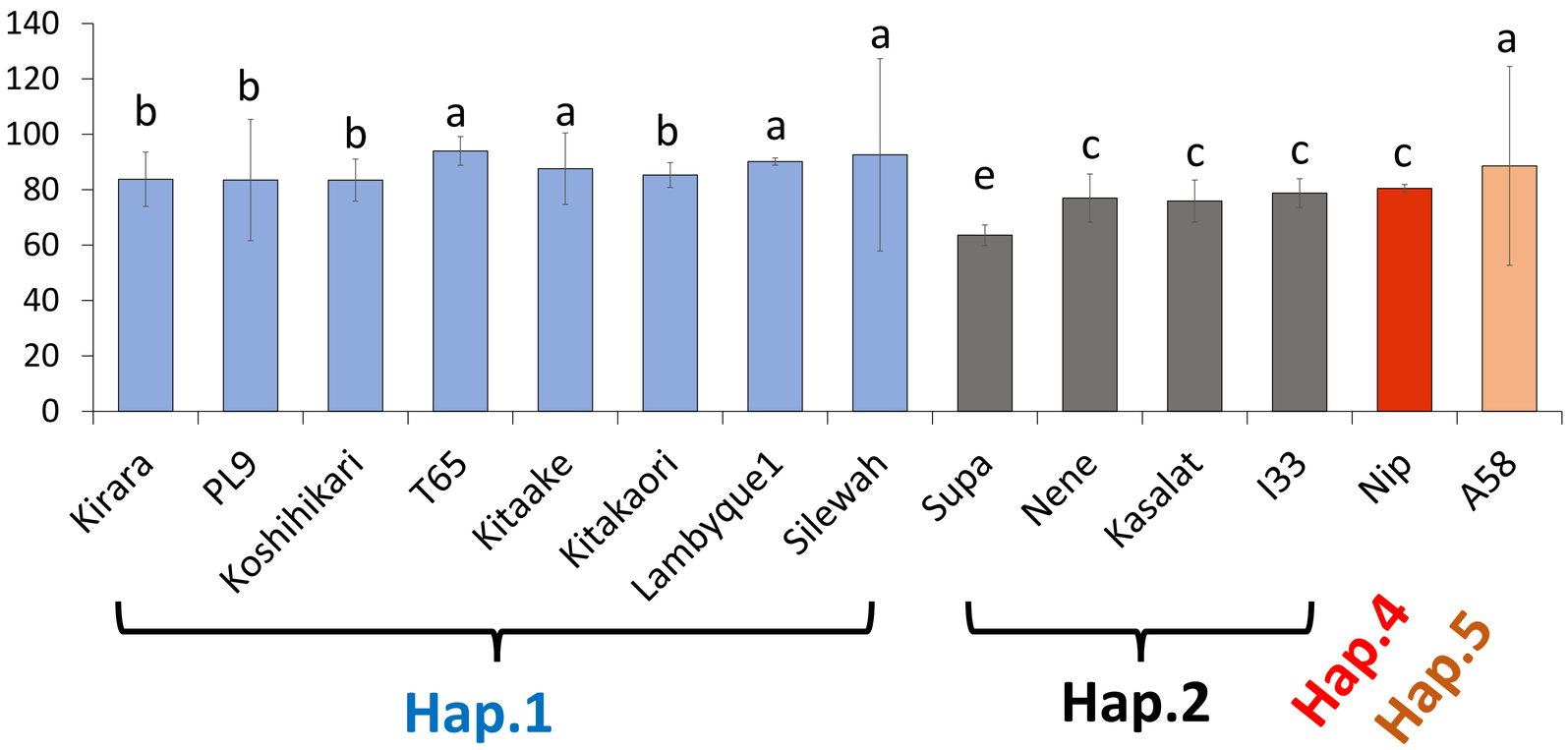

d.

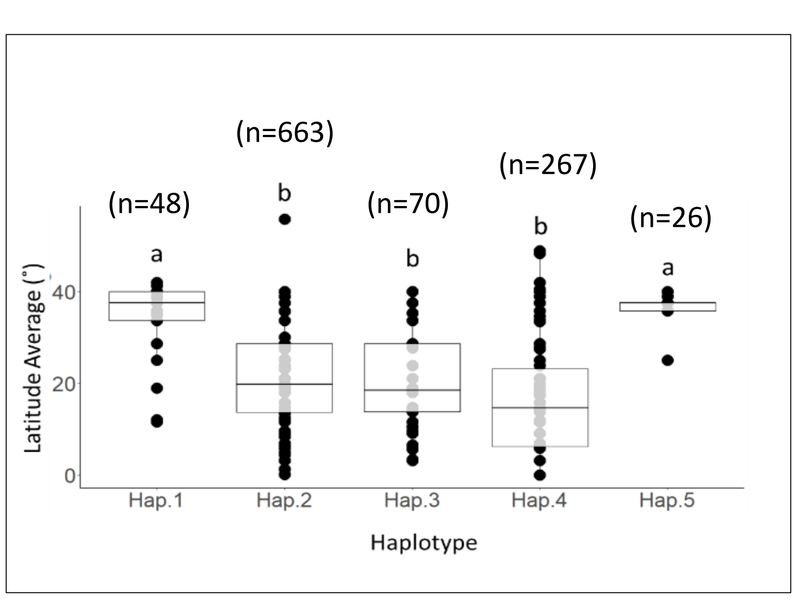

Fig. S5 Haplotype variation of *OsGELP87*. (a) SNP polymorphisms among major haplotypes in the 2-kb promoter region of *OsGELP87*. A total of 18 SNPs (right to left) are shown as black bars, and the red box indicates the sgRNA target position. Notably, no SNP polymorphisms were detected between Hap.1 and Hap.4 within the 2-kb promoter region. **(b)** SNP variation across the *OsGELP87* locus among selected rice accessions. Each row represents a rice accession, and each column corresponds to a SNP position relative to the IRGSP-1.0 reference genome. Colored cells indicate nucleotide differences compared with the reference. Accessions are grouped into haplotypes (Hap.1, Hap.2, Hap.4, Hap.5), with corresponding pollen fertility values (%) shown on the right. **(c)** Pollen fertility (%) of representative rice accessions grown under greenhouse (GH) conditions in Hokkaido, a high-latitude region. Bars show mean fertility, and different letters denote statistically significant differences ($P < 0.05$). Accessions carrying Hap.1 exhibit high pollen fertility, whereas Hap.2, Hap.4, and Hap.5 show reduced fertility under the same growth conditions. **(d)** Latitude averages each haplotype based on Rice SNP-Seek database data. The groups letters indicated the significant level based on Duncan's Test.

Fig. S6 Multiple sequence alignment of OsGELP87 haplotypes showing conserved motifs and functional domains. Amino acid sequence alignment of five OsGELP87 haplotypes (Hap.1–Hap.5) highlights conserved functional regions. The **yellow box** indicates the *signal peptide* sequence, while **gray-shaded regions** represent the four conserved *GDSL lipase motifs* characteristic of GDSL-type lipases. The **magenta-highlighted region** marks the **S-pamitolayton (Serine active site)**, which is part of the catalytic triad essential for enzymatic activity. Asterisks (*) denote identical amino acids among all haplotypes.

a. Hap.1

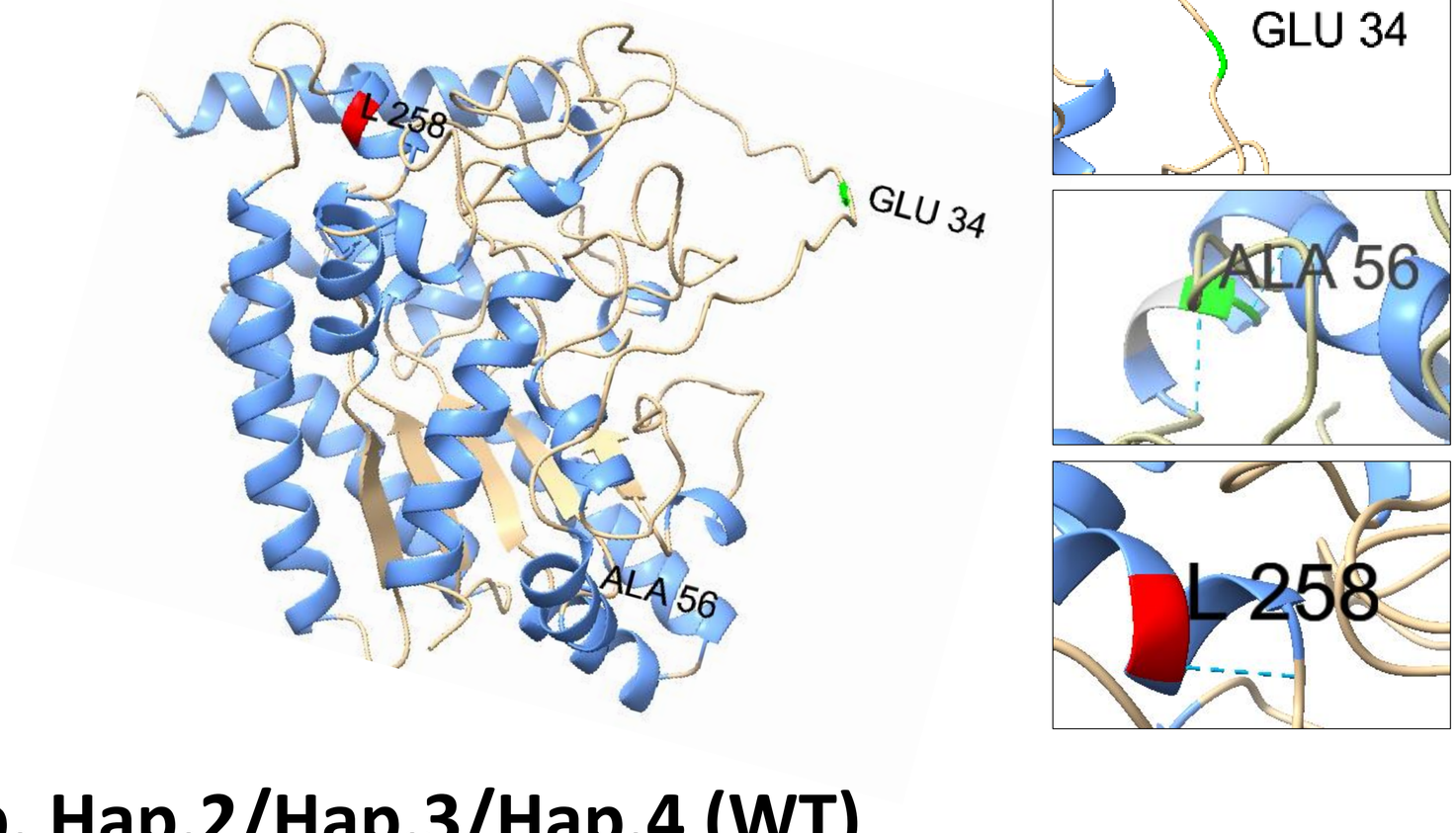

b. Hap.2/Hap.3/Hap.4 (WT)

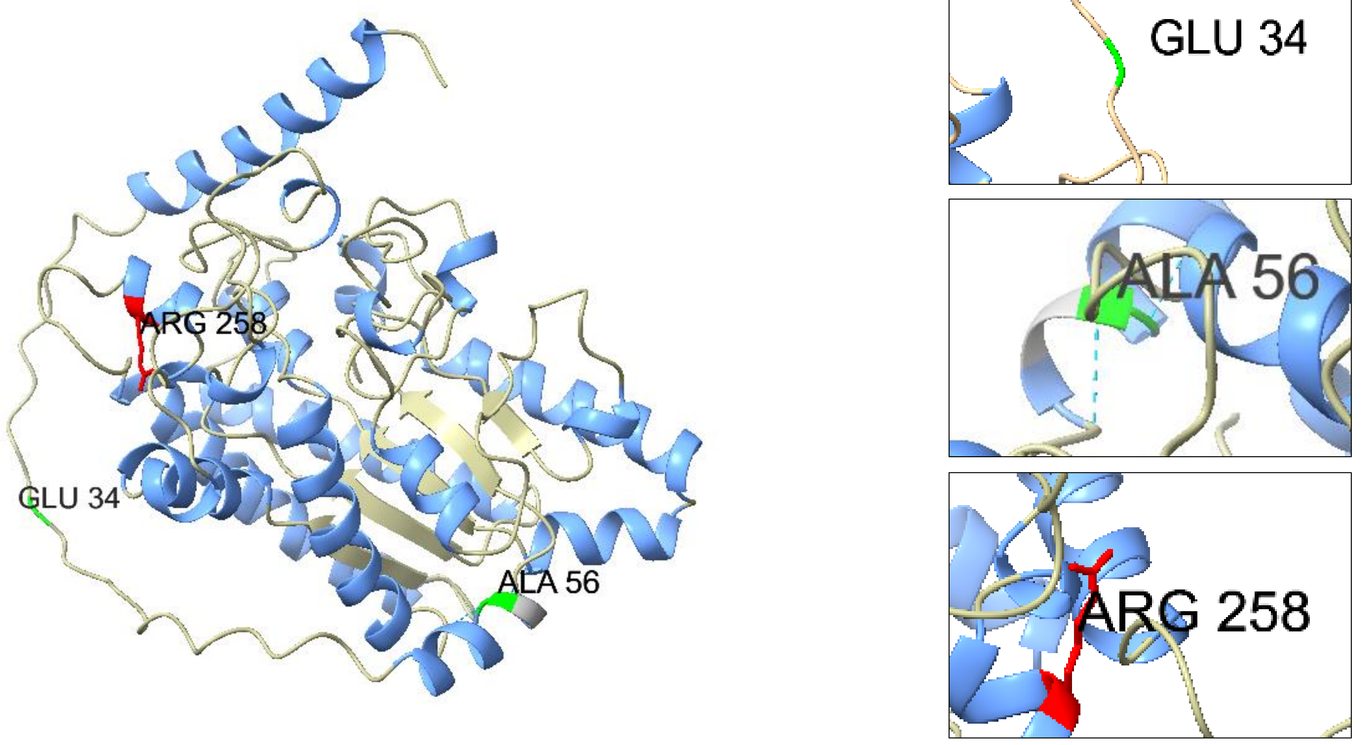

c. Hap.5

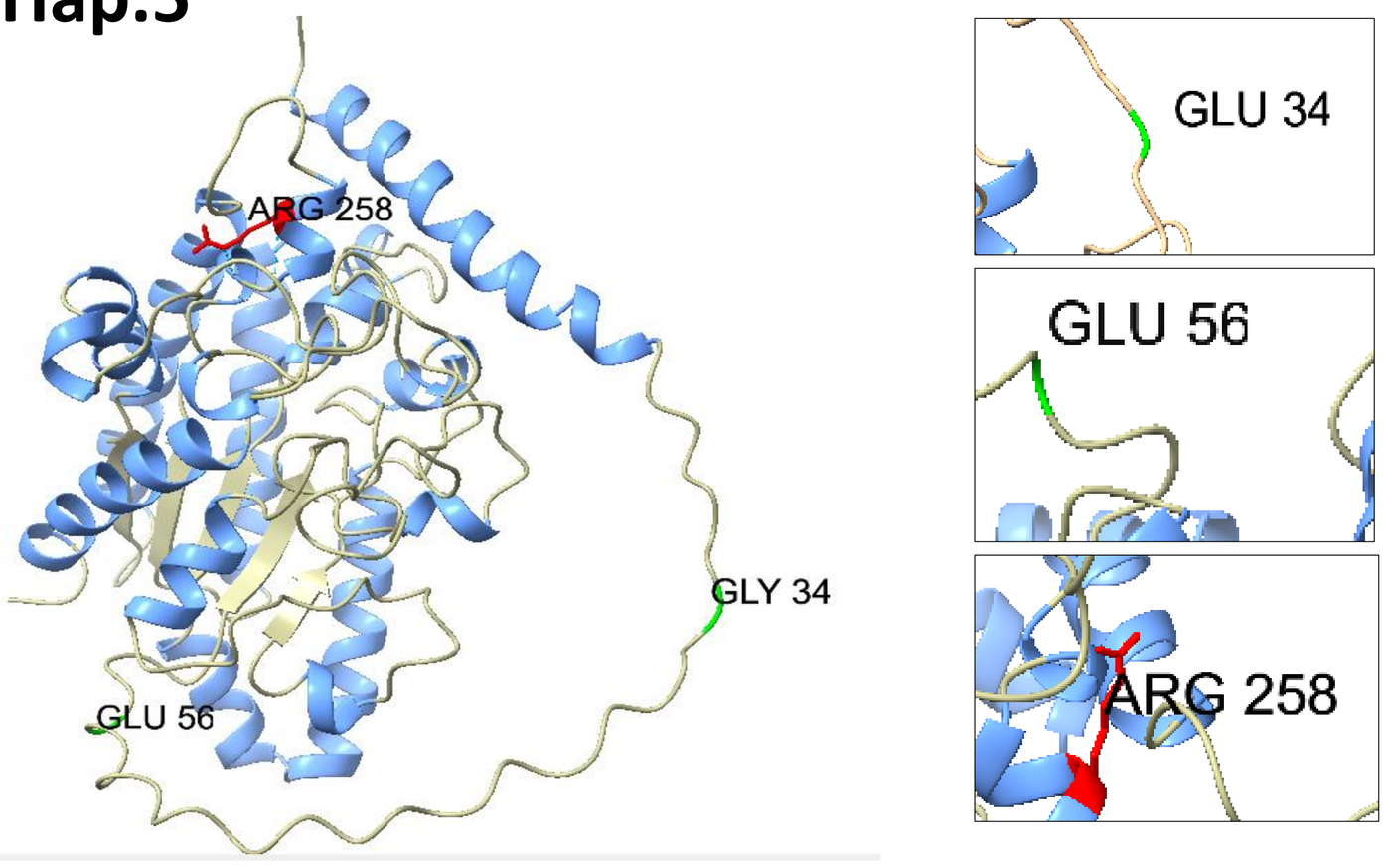

Fig. S7 Predicted three-dimensional structures of *OsGELP87* haplotypes showing amino acid variations at key functional residues. (a) *OsGELP87* Hap.1, **(b)** *OsGELP87* Hap.2/Hap.3/Hap.4 (wild type), and **(c)** *OsGELP87* Hap.5. Protein structures were predicted using AlphaFold and visualized in PyMOL. The overall folding pattern corresponds to the conserved α/β-hydrolase architecture typical of GDSL-type lipases, consisting of central β-sheets surrounded by α-helices (blue) connected by loops (beige). Key variant residues are shown as stick models: **Glu34**, **Ala56 (or Glu56)**, and **Arg258**. Enlarged panels (right) depict the local environment and potential hydrogen bond interactions around each residue.

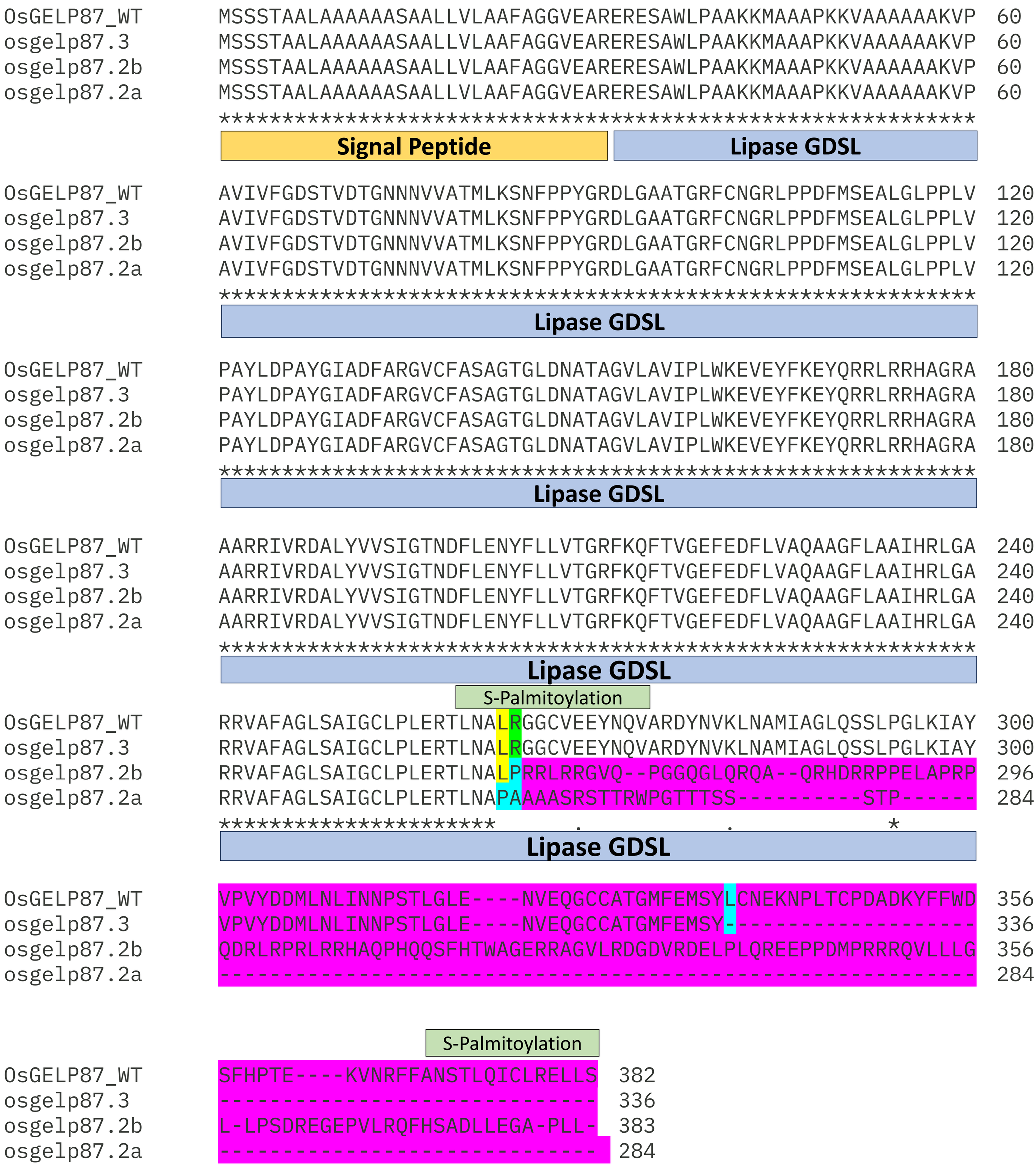

Fig. S8 Sequence alignment of OsGELP87 wild-type and mutant proteins.
Multiple sequence alignment of *OsGELP87* wild type (WT) and mutant alleles (*osgelp87.3*, *osgelp87.2b*, and *osgelp87.2a*). Conserved residues are indicated by asterisks. Functional regions are annotated: signal peptide (orange), GDSL lipase motifs (blue), and predicted S-palmitoylation sites (green). Magenta highlights indicate truncations or deletions in mutant variants relative to WT.

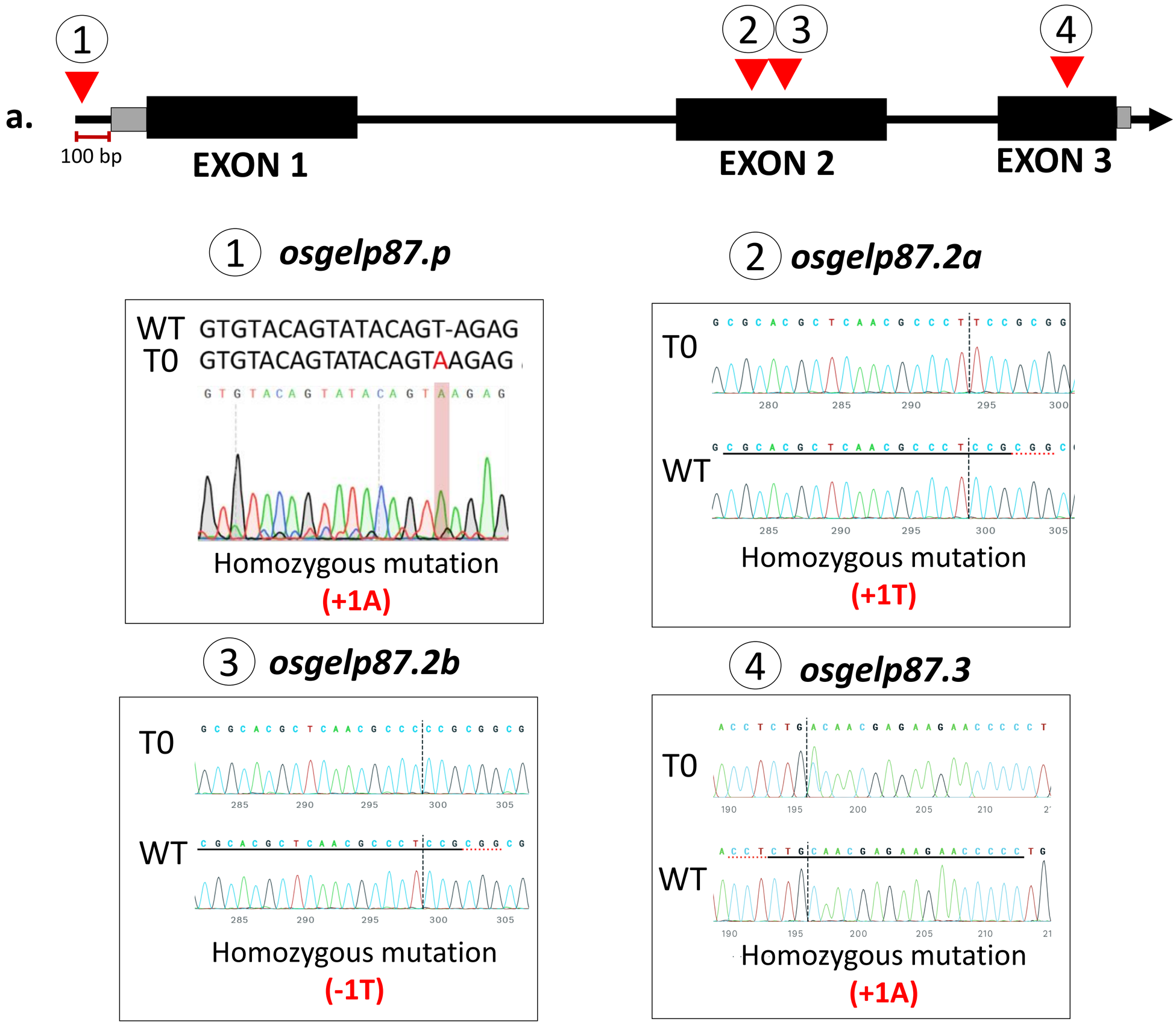

Fig. S9 Generation and phenotypic analysis of *osgelp87* mutants. (a) Schematic representation of the *OsGELP87* gene structure and CRISPR/Cas9 target sites. Red arrowheads indicate the positions of the four CRISPR target sites located in exons 1, 2, and 3. DNA sequencing chromatograms of wild-type (WT) and representative homozygous mutants show different insertion/deletion (indel) mutations: *osgelp87.p* (+1A), *osgelp87.2a* (+1T), *osgelp87.2b* (–1T), and *osgelp87.3* (+1A). All mutations introduced frameshifts predicted to disrupt *OsGELP87* function. **(b)** Pollen fertility analysis of WT and *osgelp87* mutants. WT plants showed normal pollen fertility (~85–90%), while all mutant alleles exhibited significantly reduced pollen fertility. Among them, *osgelp87.2b* showed the most severe reduction (***$p < 0.001$), followed by *osgelp87.3* and *osgelp87.p* (**$p < 0.01$), and *osgelp87.2a* (*$p < 0.05$).

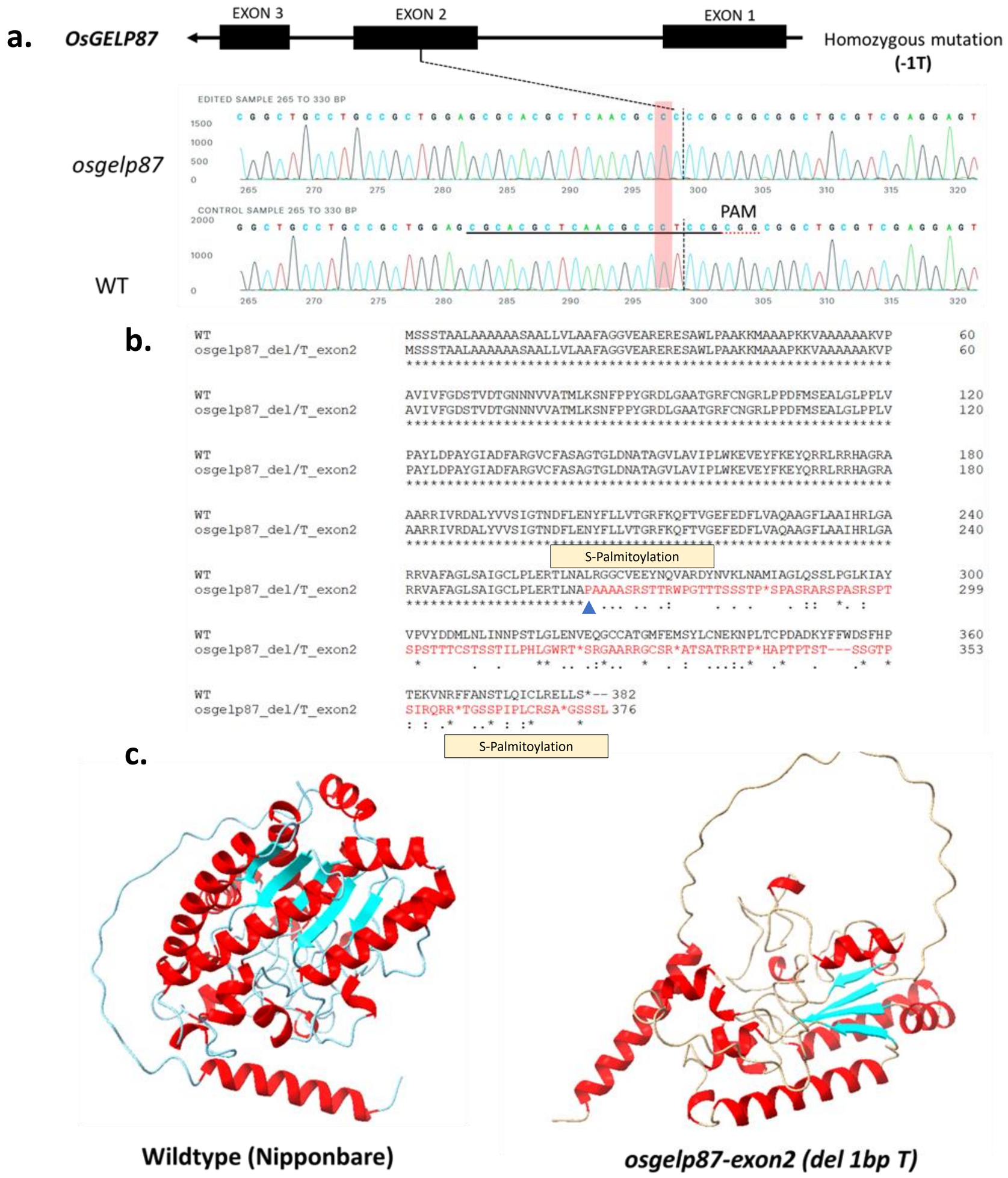

Fig. S10 Mutant *osgelp87.2a* **(a)** Gene models of *OsGELP87* and Sanger sequence of mutation. Underline indicates the 20-bp-long target sites beside the PAM sequence (CCT), which guides the Cas9 enzyme. Green boxes indicate the corresponding target sites after mutation induction. Red box indicated the target region for CRISPR/Cas9-induced mutation. **(b)** Alignment of amino acid sequence of wildtyoe and *osgelp87-exon2* mutant. Blue text highlight was indicated the amino acid change start. **(c) Protein structure difference** between wildtype and mutant *osgelp-exon2 (del 1bp T).* The red and yellow color showed the alpha helixes and blue color showed the beta sheet. The green color showed the two of alpha sheet that disappeared in mutant, orange color showed the signal peptide sequence. The mutant was losing 5 alpha helix and one beta sheet

a.

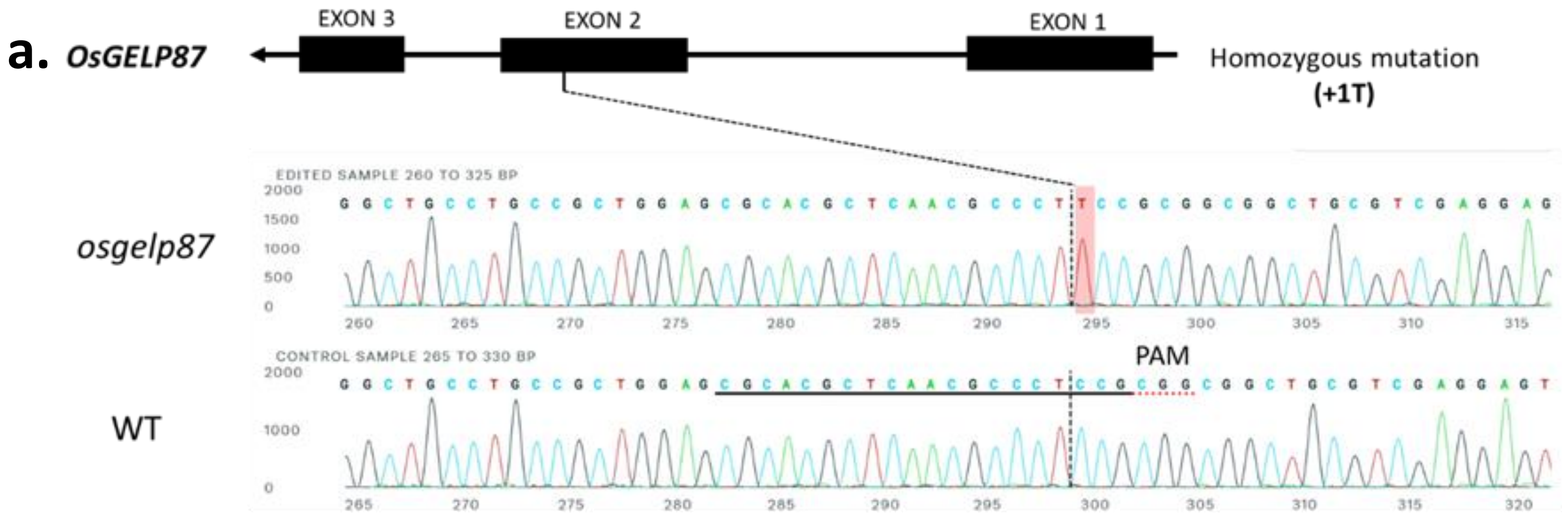

b.

```
osgelp87_EXON2_inT      MSSSTAALAAAAAASAALLVLAAFAGGVEARERESAWLPAAKKMAAAPKKVAAAAAAKVP  60
OsGELP87                MSSSTAALAAAAAASAALLVLAAFAGGVEARERESAWLPAAKKMAAAPKKVAAAAAAKVP  60
                        ************************************************************

osgelp87_EXON2_inT      AVIVFGDSTVDTGNNNVVATMLKSNFPPYGRDLGAATGRFCNGRLPPDFMSEALGLPPLV  120
OsGELP87                AVIVFGDSTVDTGNNNVVATMLKSNFPPYGRDLGAATGRFCNGRLPPDFMSEALGLPPLV  120
                        ************************************************************

osgelp87_EXON2_inT      PAYLDPAYGIADFARGVCFASAGTGLDNATAGVLAVIPLWKEVEYFKEYQRRLRRHAGRA  180
OsGELP87                PAYLDPAYGIADFARGVCFASAGTGLDNATAGVLAVIPLWKEVEYFKEYQRRLRRHAGRA  180
                        ************************************************************

osgelp87_EXON2_inT      AARRIVRDALYVVSIGTNDFLENYFLLVTGRFKQFTVGEFEDFLVAQAAGFLAAIHRLGA  240
OsGELP87                AARRIVRDALYVVSIGTNDFLENYFLLVTGRFKQFTVGEFEDFLVAQAAGFLAAIHRLGA  240
                        ************************************************************
                                                S-Palmitoylation
osgelp87_EXON2_inT      RRVAFAGLSAIGCLPLERTLNALPRRLRRGVQPGGQGLQRQAQ----RHDRRPPEL----  292
OsGELP87                RRVAFAGLSAIGCLPLERTLNALRGGCVEEYNQVARDYNVKLNAMIAGLQSSLPGLKIAY  300
                        **********************     .  :  .:. : : :      :   * *

osgelp87_EXON2_inT      APRPQDRLRPRLRRHAQPHQQSFHTWAGERRAGVLRDGDVRDELPLQREEPPDMPRRRQV  352
OsGELP87                VPVYDDML----NLINNPSTLGLE----NVEQGCCATGMFEMSYLCNEKNPLTCPDADKY  352
                        .*  :* *    .   :*   .:.    : . *    * .. .   :.::*   *   :

osgelp87_EXON2_inT      LLLGL-LPSDREGEPVLRQFHSADLLEGA-PLL-  383
OsGELP87                FFWDSFHPTE----KVNRFFANSTLQICLRELLS  382
                        :: .   *::     * * * .: *      **
                                S-Palmitoylation
```

c.

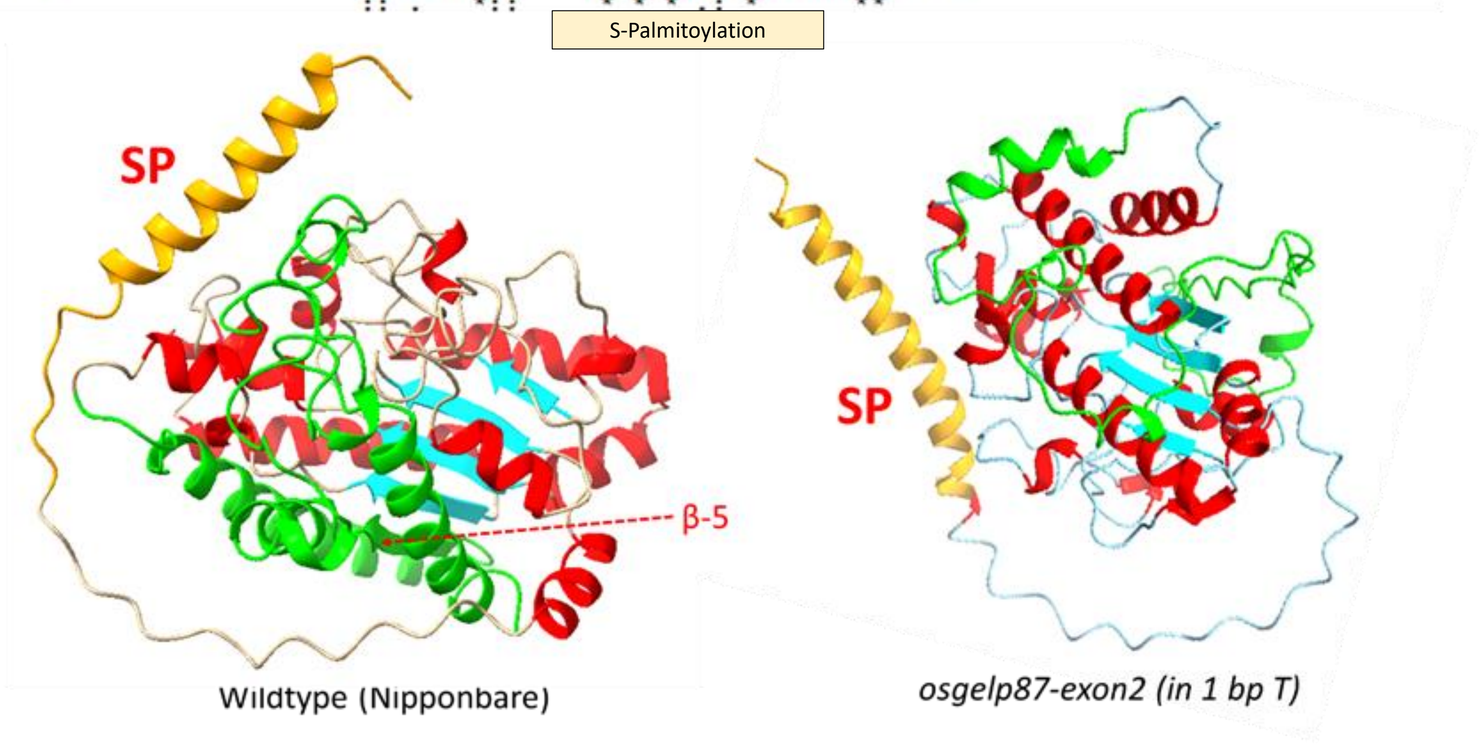

Fig. S11 Mutant *osgelp87.2b* (a) Gene models of *OsGELP87* and Sanger sequence of mutation. Underline indicates the 20-bp-long target sites beside the PAM sequence (CCT), which guides the Cas9 enzyme. Green boxes indicate the corresponding target sites after mutation induction. Red box indicated the target region for CRISPR/Cas9-induced mutation. **(b)** Alignment of amino acid sequence of wildtyoe and *osgelp87-exon2* mutant. Blue text highlight was indicated the amino acid change start. **(c) Protein structure difference** between wildtype and mutant *osgelp-exon2 (in 1bp T).* The red and yellow color showed the alpha helixes and blue color showed the beta sheet. The green color showed the two of alpha sheet that disappeared in mutant, orange color showed the signal peptide sequence. The mutant was losing 5 alpha helix and one beta sheet

a.

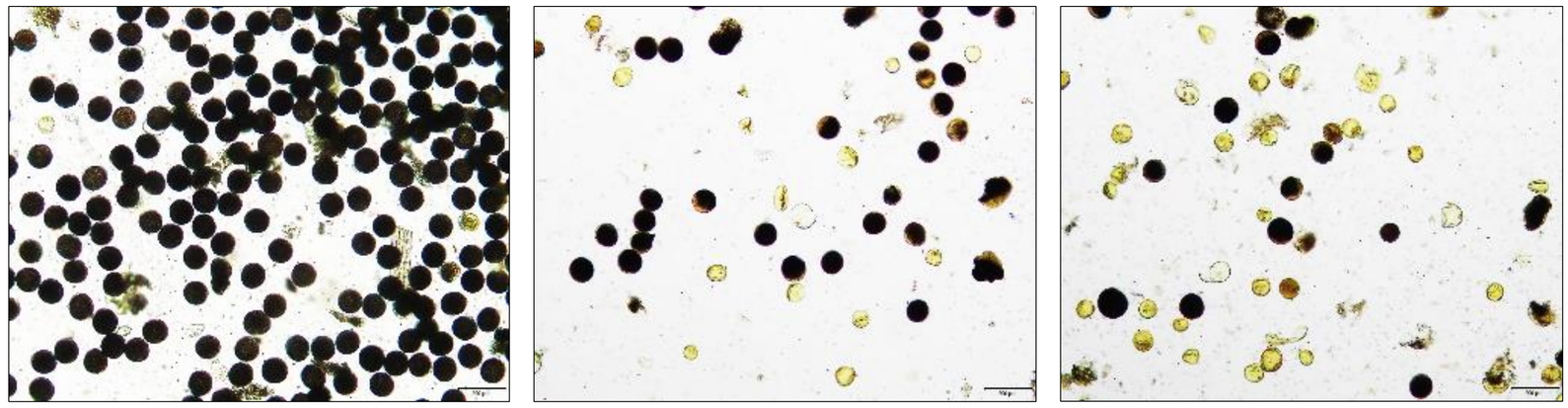

b.

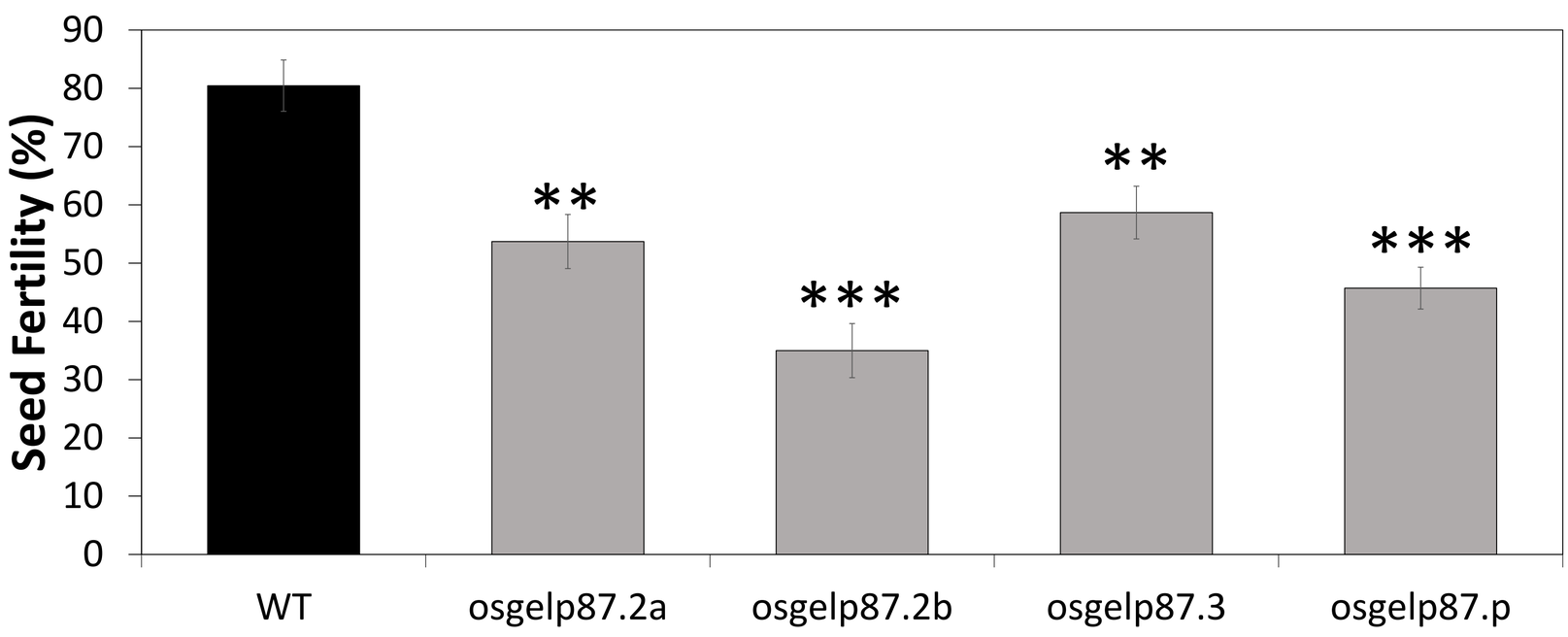

c.

Fig. S12 Reduced pollen fertility and seed set in *osgelp87* mutants. (a) Pollen fertility of wild type (WT) and *osgelp87* mutant lines (*osgelp87.2a*, *osgelp87.2b*, *osgelp87.3*, and *osgelp87.p*) assessed by 1% I_2–KI staining. Darkly stained pollen grains indicate fertile pollen, whereas lightly stained or unstained grains indicate aborted pollen. Percentages below each image represent pollen fertility. **(b)** Seed fertility of WT and *osgelp87* mutants. Values represent means ± SD (n ≥ 3 biological replicates). Asterisks indicate significant differences compared with WT (**P < 0.01, ***P < 0.001; Student's *t*-test). **(c)** Representative panicles of WT and *osgelp87* mutant plants showing reduced seed set in mutants. Scale bar = 5 cm

a.

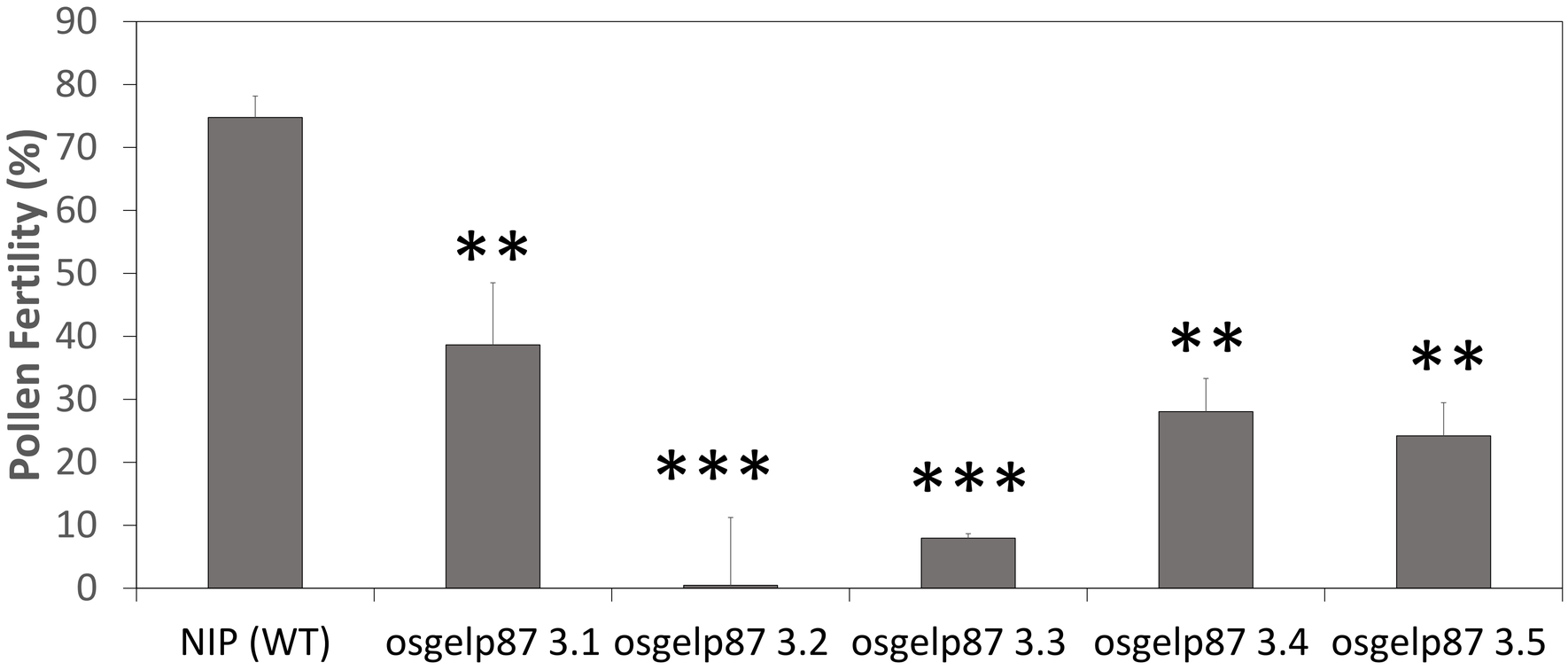

b.

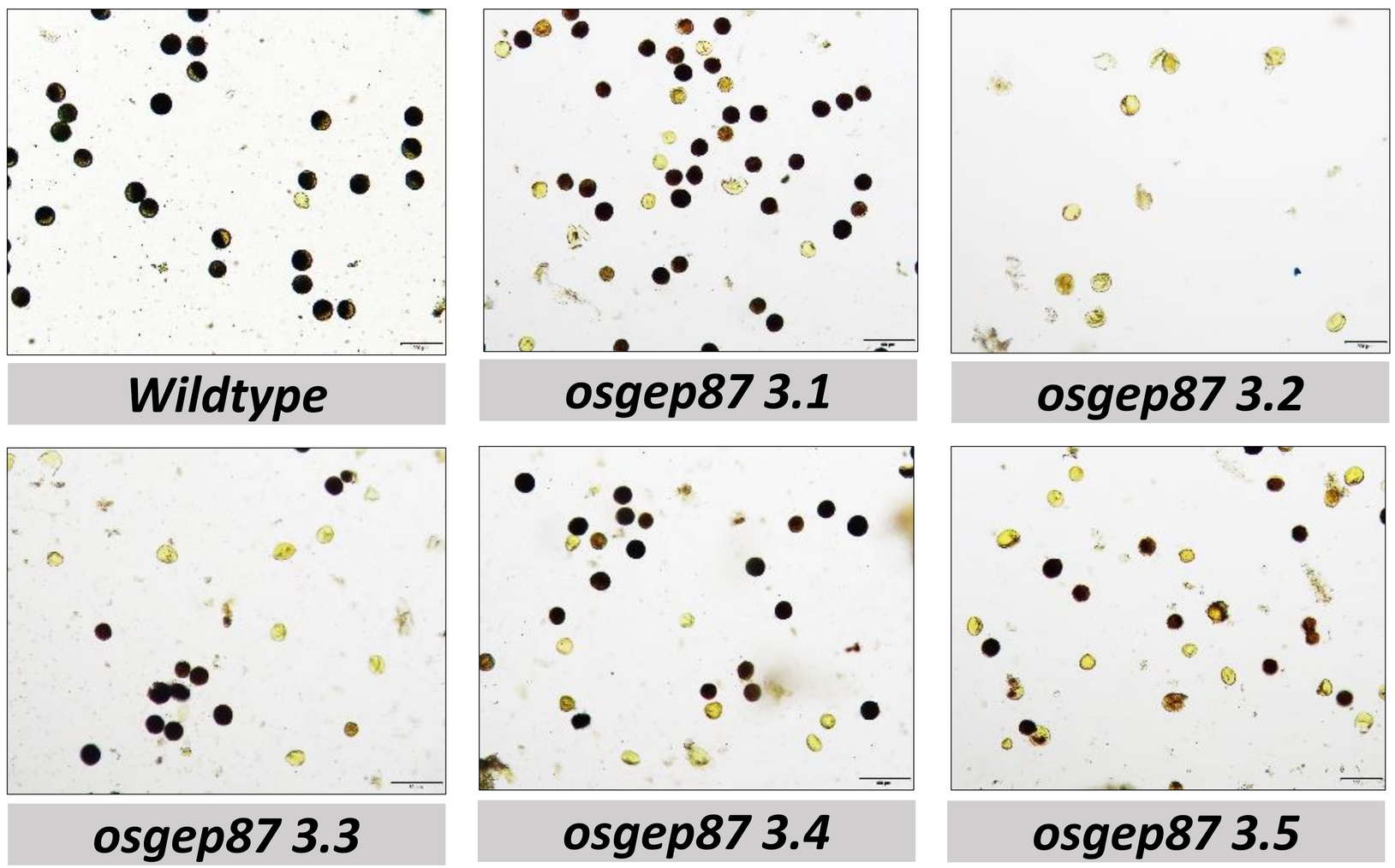

c.

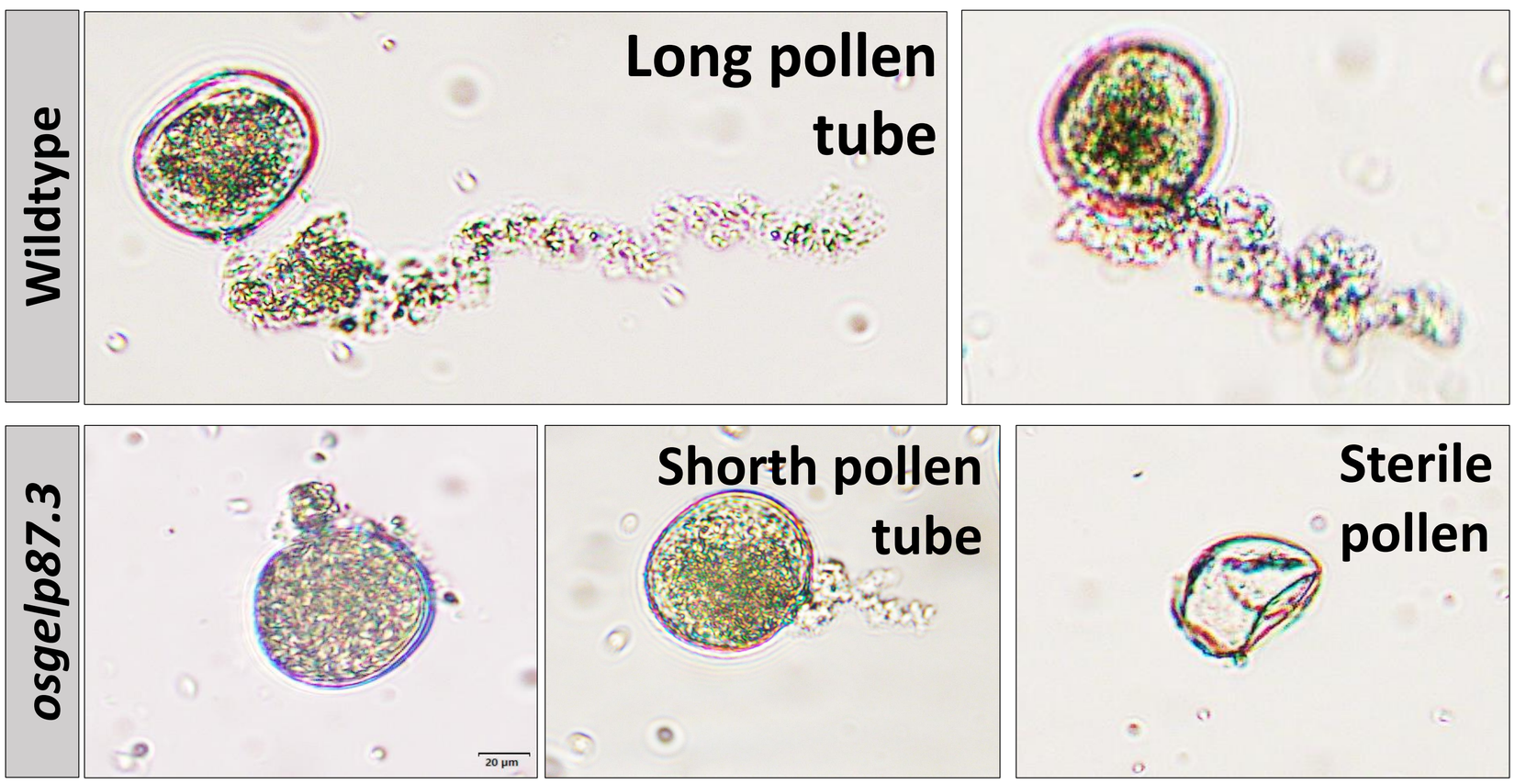

Fig. S13 Pollen fertility analysis in *osgelp87-3* mutant lines. (a) Pollen fertility percentage in wild type (NIP) and *osgelp87-3* independent mutant lines (3.1–3.5). Data are presented as mean ± SE. Asterisks indicate significant differences compared to the wild type based on Duncan's test (**P < 0.01; ***P < 0.001**). **(b)** I_2–KI staining of mature pollen grains showing the proportion of fertile (darkly stained) and sterile (unstained or lightly stained) pollen in wild type and *osgelp87-3* mutants. Scale bars = 100 µm. **(c)** In vitro pollen germination assay showing pollen tube growth in wild type and *osgelp87-3* mutants. Wild type pollen produced long pollen tubes, whereas *osgelp87-3* mutants exhibited short or no pollen tube formation, and some pollen grains appeared sterile. Scale bars = 20 µm

a.

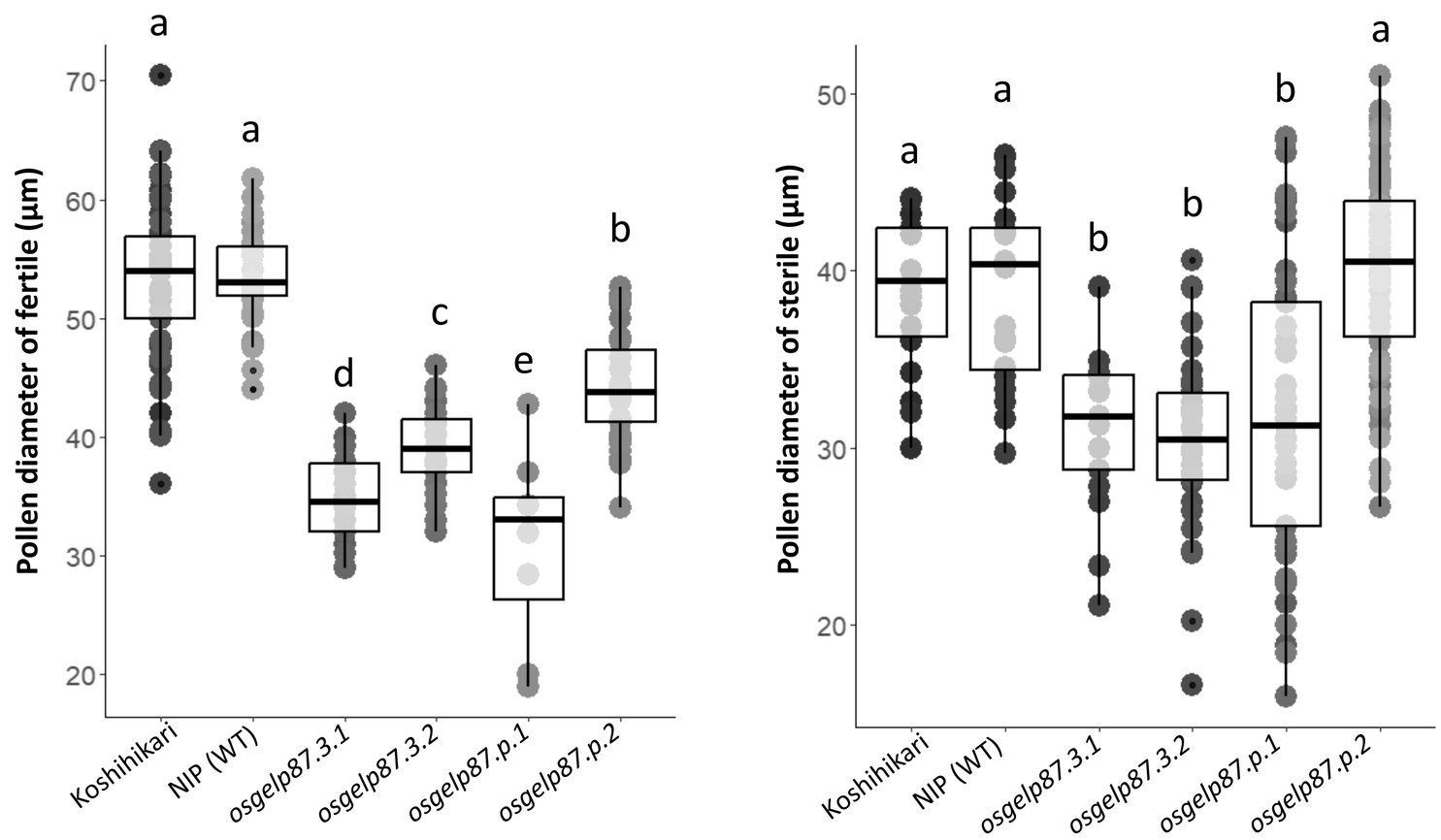

b.

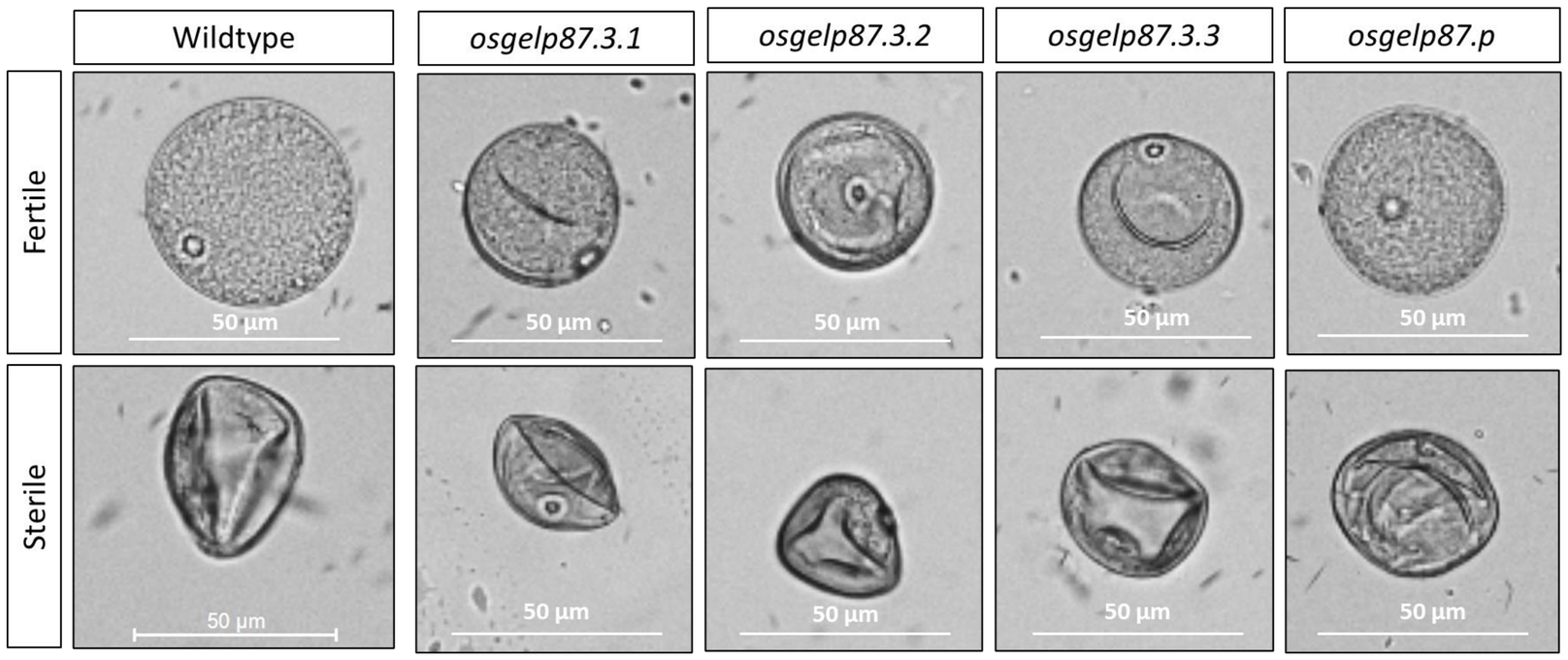

Fig. S14 Comparison of pollen grain diameter among different genotypes.
(a) Pollen diameter in fertile pollen across koshihikari, wild-type (Nipponbare/NIP), and OsGELP87 mutant lines. Groups labelled with different letters (a–e) indicate statistically significant differences ($p < 0.05$, ANOVA followed by Tukey's HSD test). Mutant lines show significantly reduced pollen diameter compared to the wildtype and transgenic plants. **(b)** Sterile pollen diameter among the same genotypes. Mutant lines exhibit significantly smaller sterile pollen compared to wildtype or transgenic plants. Statistical groupings (a, b) highlight differences in sterile pollen size

a.

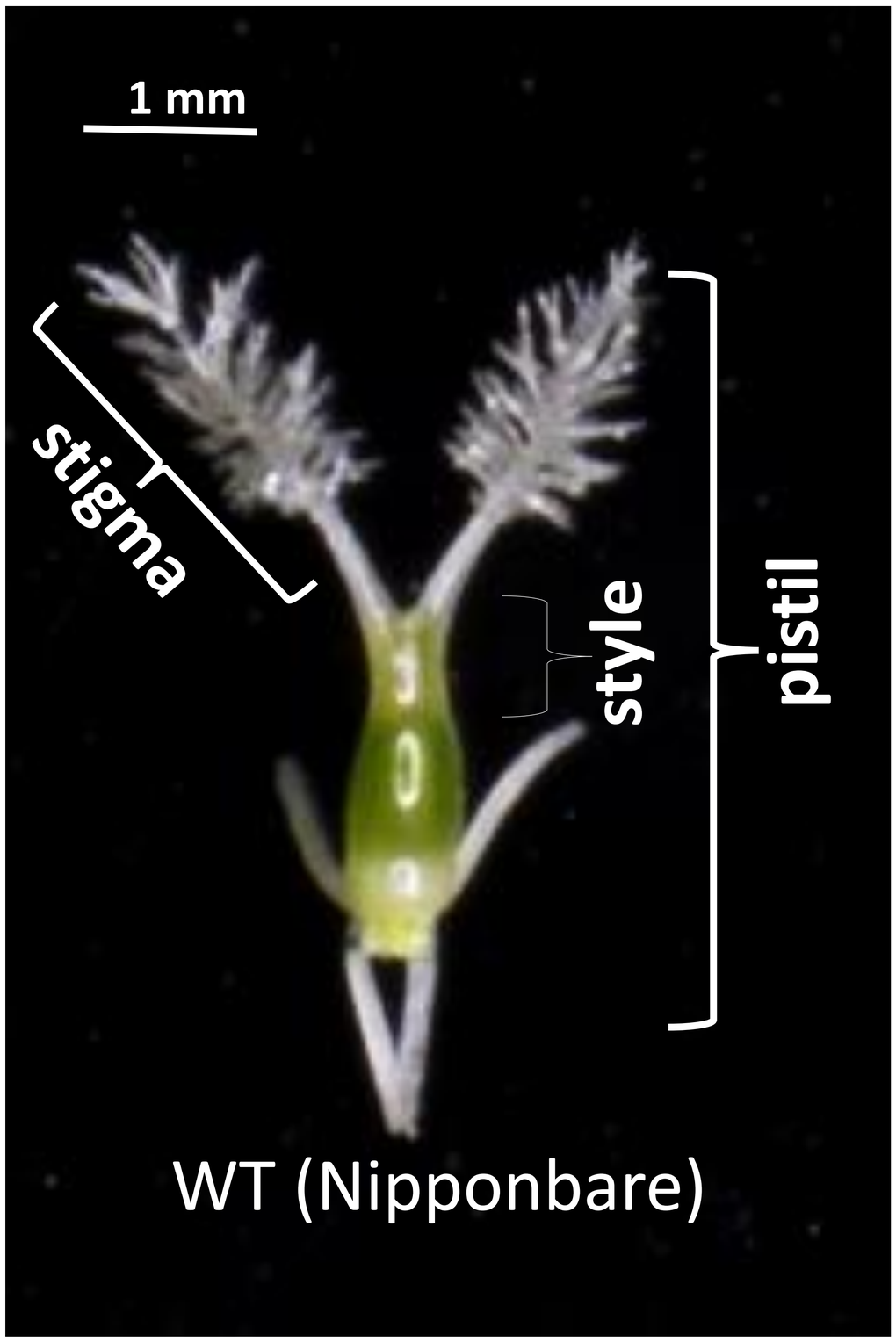

b.

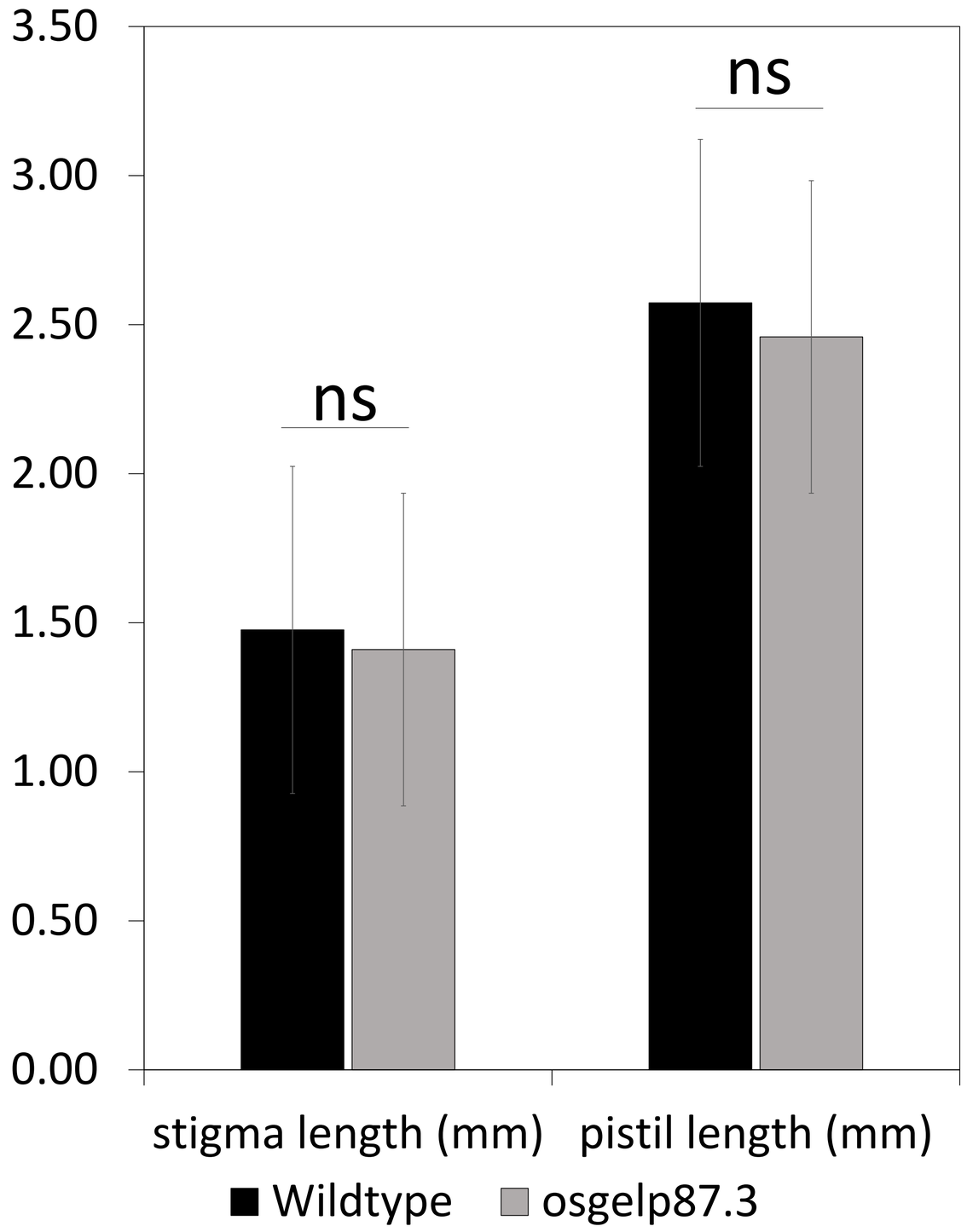

Fig. S15 Stigma and pistil morphology in wild-type and *osgelp87.3* mutant rice. (a) Morphological observation of the pistil in wild-type Nipponbare showing stigma, style, and ovary (pistil) under a stereomicroscope. Scale bar = 1 mm. **(b)** Quantification of stigma length and pistil length in wild-type (black bars) and *osgelp87.3* mutant (gray bars). No significant differences (ns) were observed between wild-type and mutant plants (Student's *t*-test)

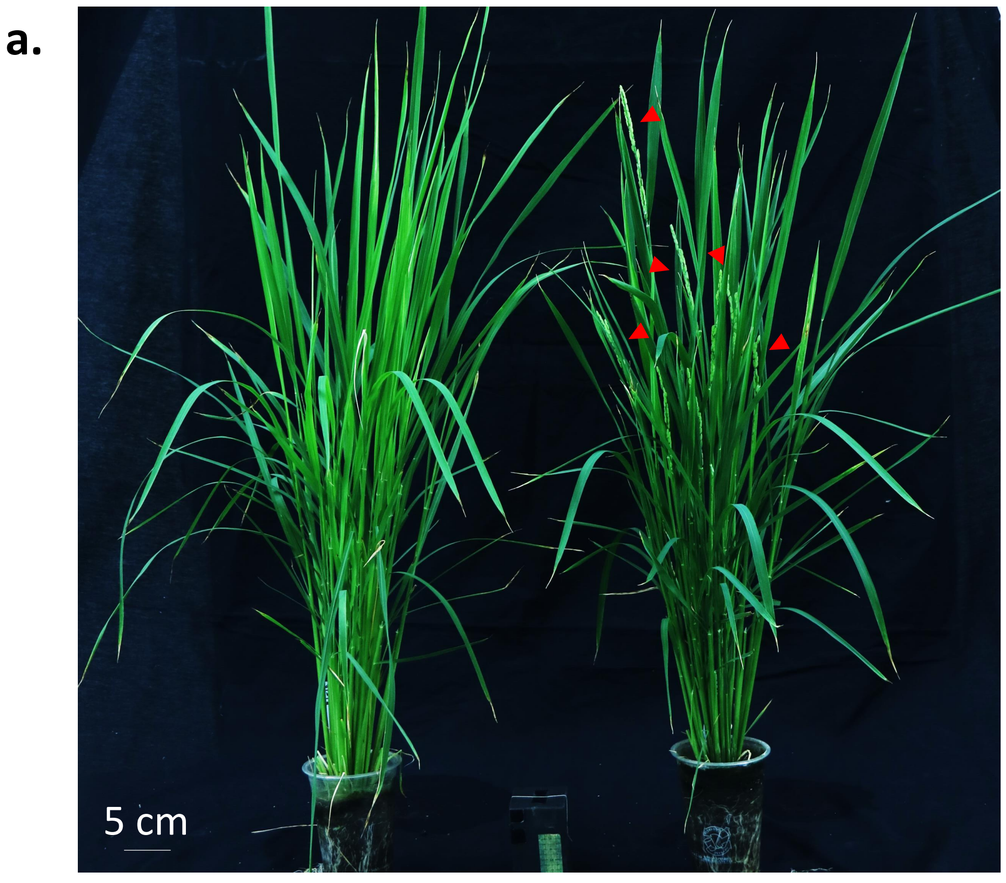

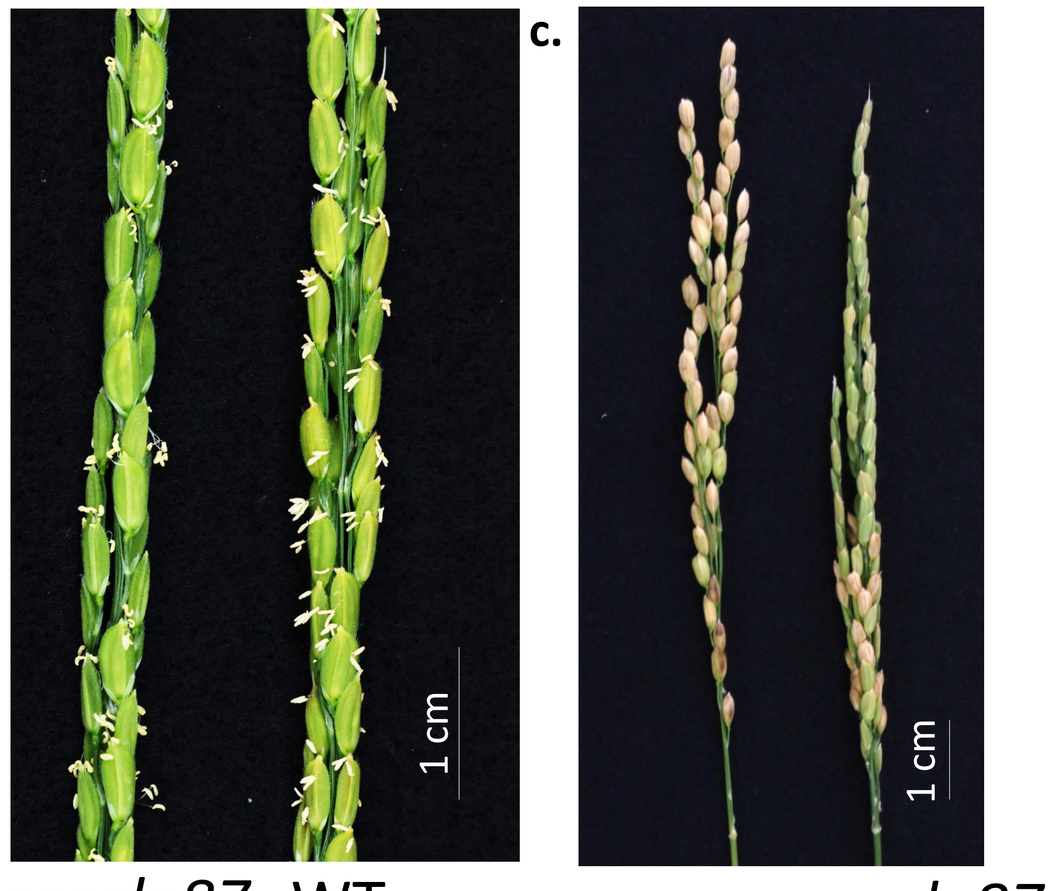

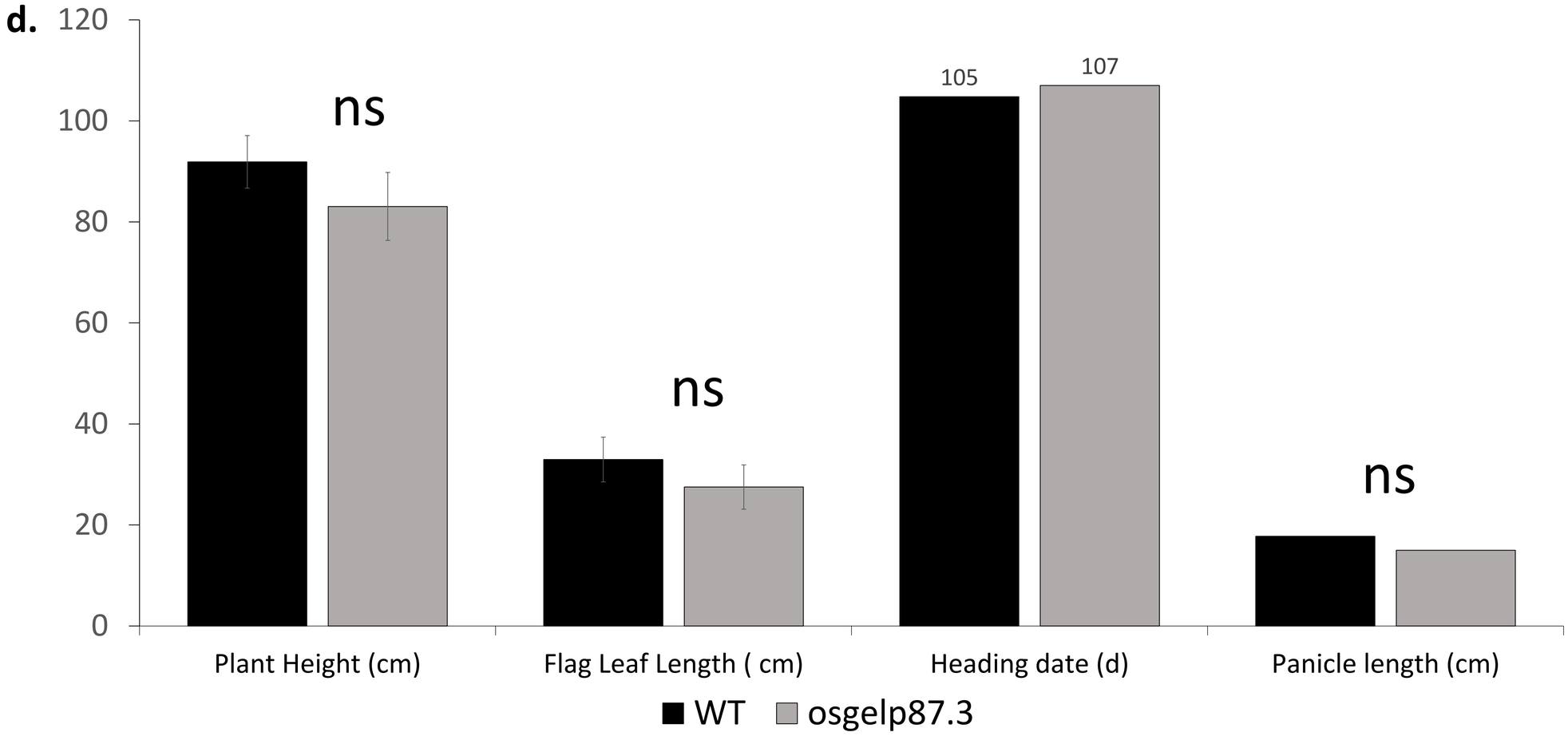

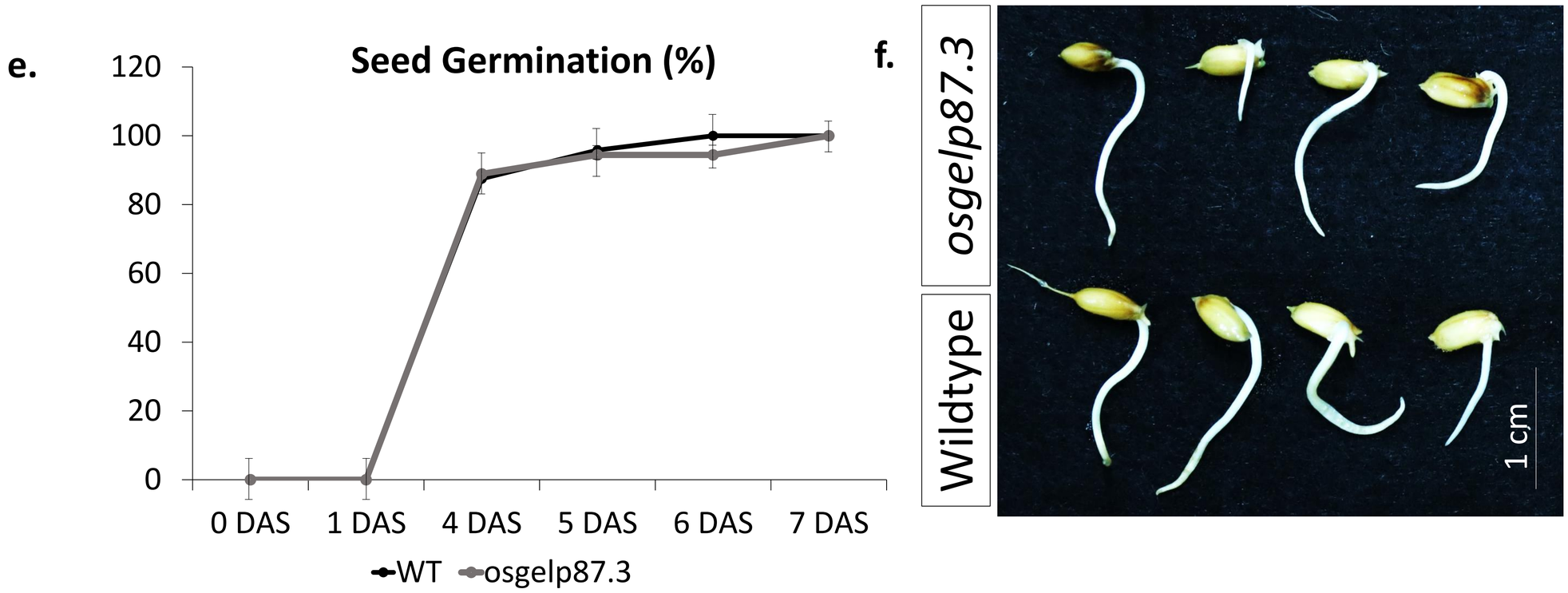

Fig. S16 Agronomic traits and seed germination analysis of the *osgelp87* mutant compared to wild-type rice. (a) Whole-plant morphology of wild-type (WT) and *osgelp87.3* at the reproductive stage. The mutant exhibits reduced tiller number and overall growth compared to WT. Scale bar = 1 cm. **(b-c)** Morphology of panicles from WT and *osgelp87.3*. The mutant shows fewer and shorter panicles. **(d)** Quantification of plant height (cm), flag leaf length (cm), heading date (days), and panicle length (cm) in WT and *osgelp87.3*. **(D)** Seed germination rate (%) from 0 to 7 days after sowing (DAS) in WT and *osgelp87.3*. **(e-f)** Representative images of germinated seeds from WT and *osgelp87.3*. Data in are presented as mean ± SE (n ≥ 3 biological replicates). Statistical significance was determined using Student's *t*-test (ns, not significant)

Fig. S17 (a) The mature seed (after oven-dried) difference between wildtype and the mutants (scale bar: 1 cm) **(b)** seed length comparison

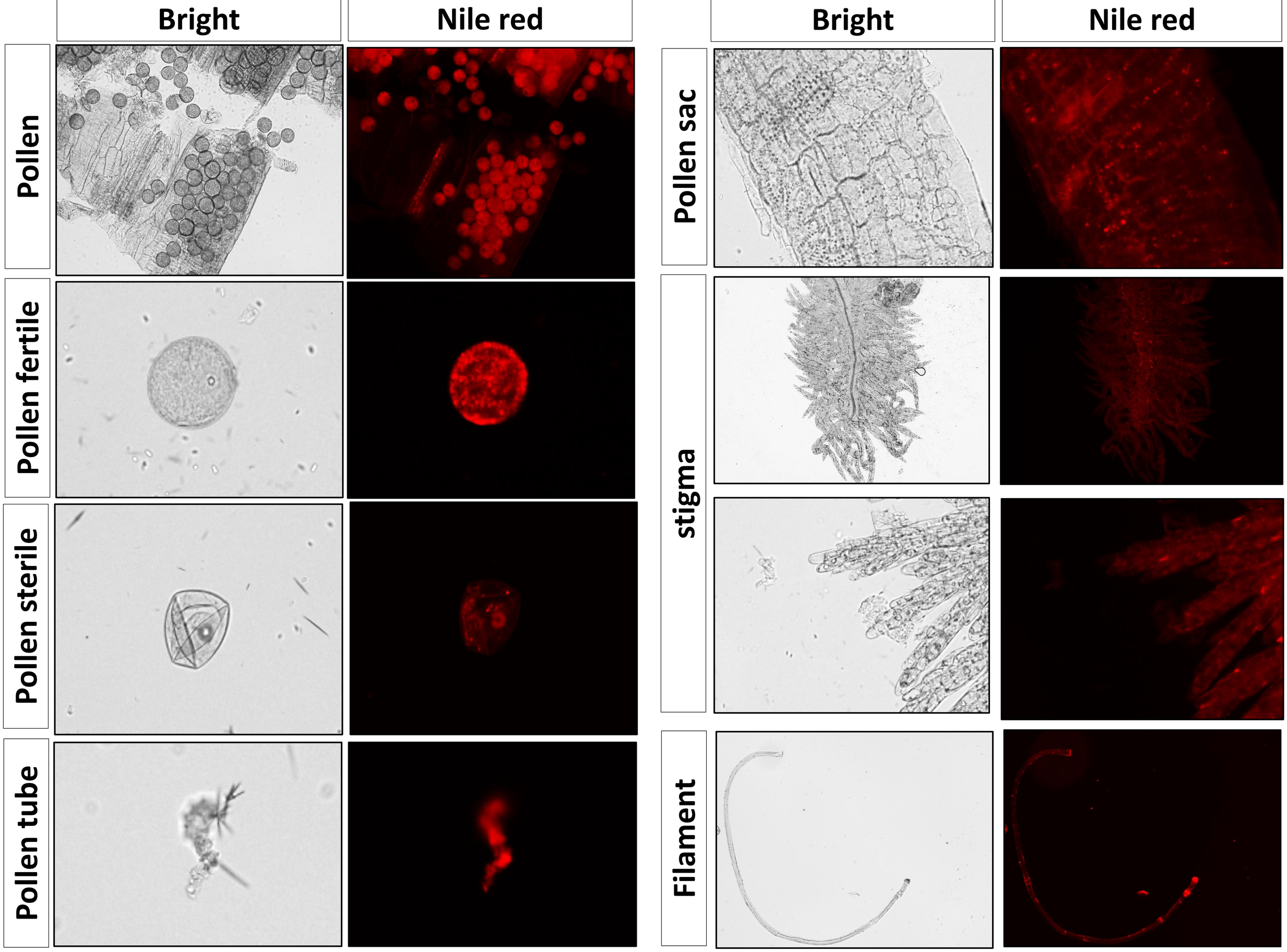

Fig. S18 Nile Red staining reveals lipid distribution in the reproductive tissues of rice (cv. Nipponbare).
Bright-field (left) and corresponding fluorescence (right) images show lipid localization in various floral tissues. Strong red fluorescence indicates the presence of neutral lipids stained by Nile Red.

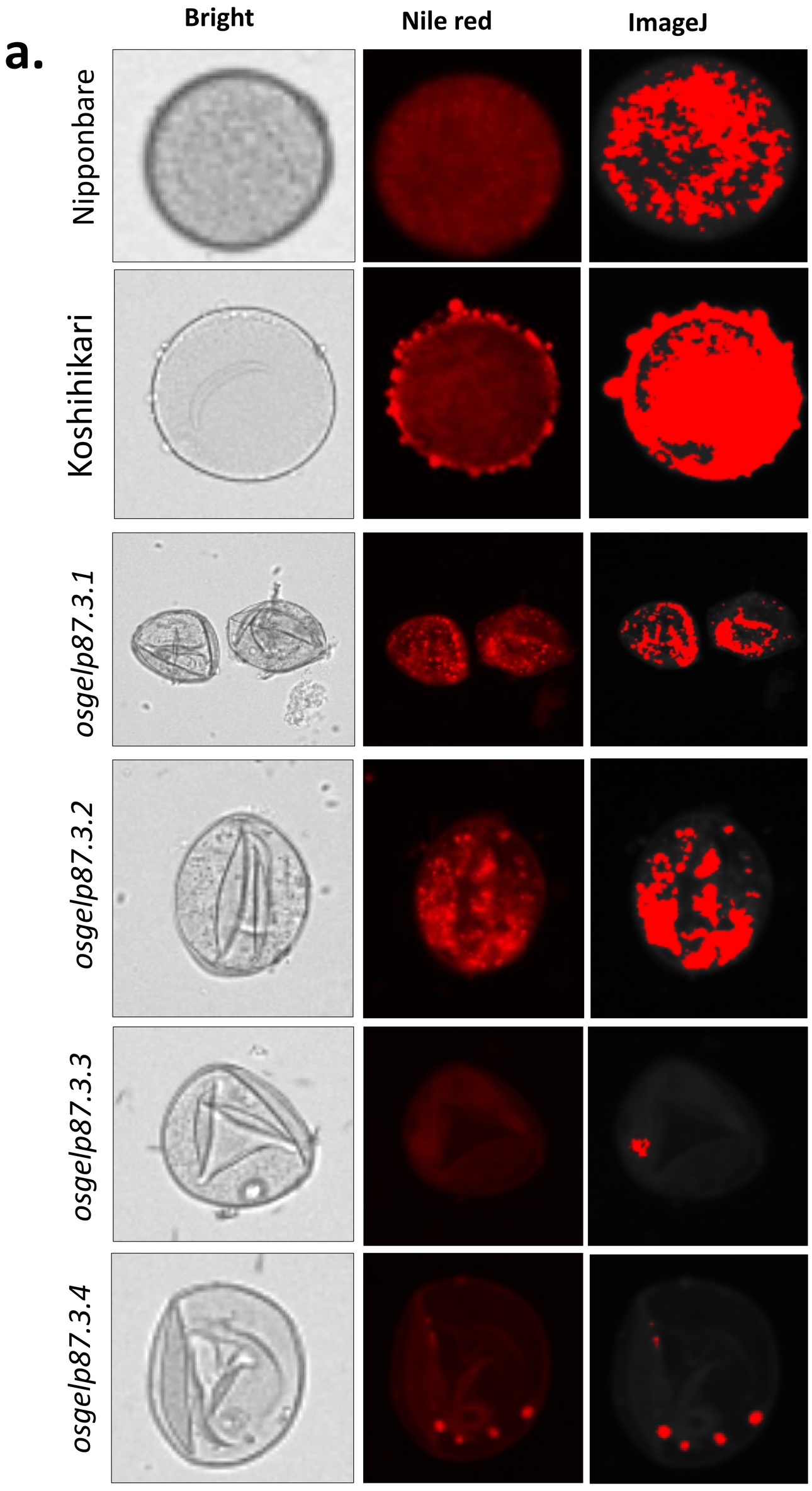

Fig. S19 (a) Analysis of lipid distribution in pollen grains using Nile red staining. Bright-field, Nile red-stained, and ImageJ-processed images of pollen grains from rice cultivars Nipponbare and Koshihikari, and OsGELP87 knockout mutants (*osgelp87.3.1*, *osgelp87.3.2*, *osgelp87*.3.3, *osgelp87*.3.4) are shown. Nile red staining reveals lipid bodies in pollen grains, visualized as red fluorescence. In wild-type Nipponbare and Koshihikari, uniform fluorescence distribution indicates intact lipid accumulation. In OsGELP87 mutants, disrupted fluorescence patterns suggest altered lipid metabolism or organization. Bright-field images provide structural context for comparison. ImageJ-processed images highlight fluorescence intensities and distributions for enhanced visualization. **(b)** lipid accumulation area and **C.** percentage of normal intine wildtype compared to mutants *osgelp87.3* and *osgelp87*.p (The Views in osgelp87p are not present in the panel).

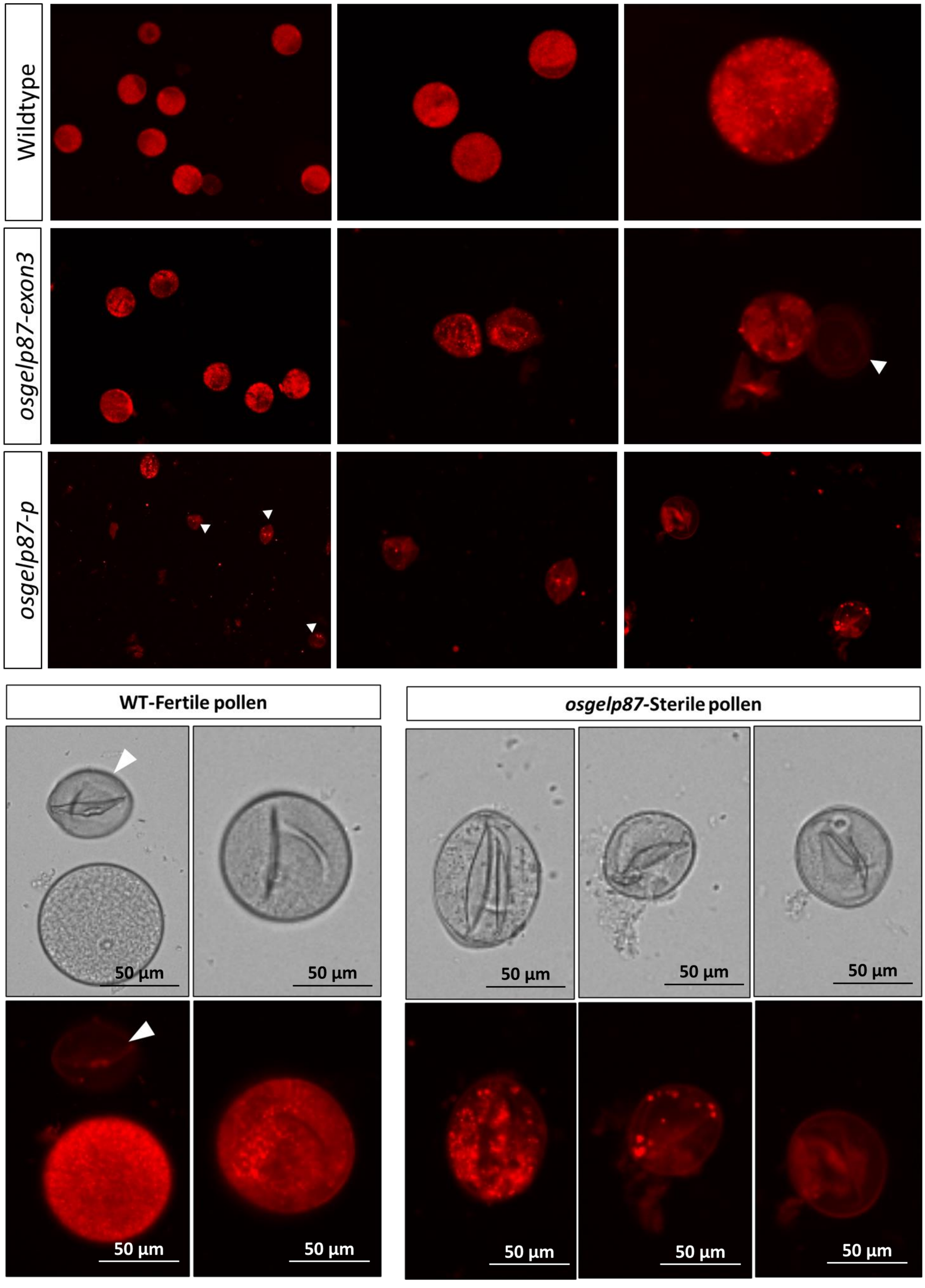

Figure S20. Nile red staining of wild-type (WT) and *osgelp87* mature pollen. Mature pollen was stained with Nile red, a dye specifically staining neutral lipids. White arrows indicate sterile pollen completely devoid of lipids.

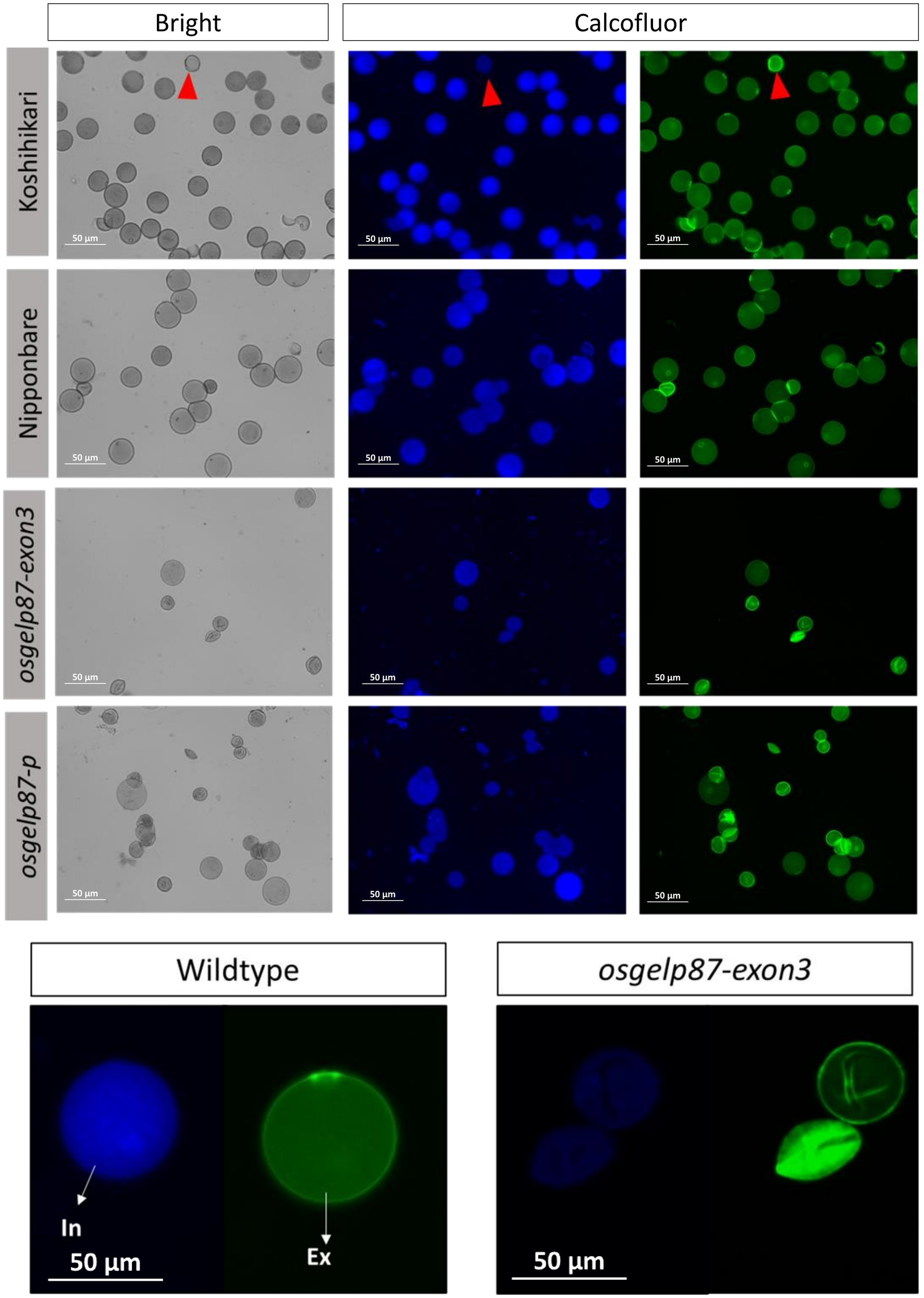

Fig. S21 Calcofluor White Staining: The different between wildtype and *osgelp87-p* mutant in pollen mature after staining. Red arrow show the pollen sterile. **Calcofluor White (CFW)** staining is a fluorescent dye technique to visualize plant **cell walls**

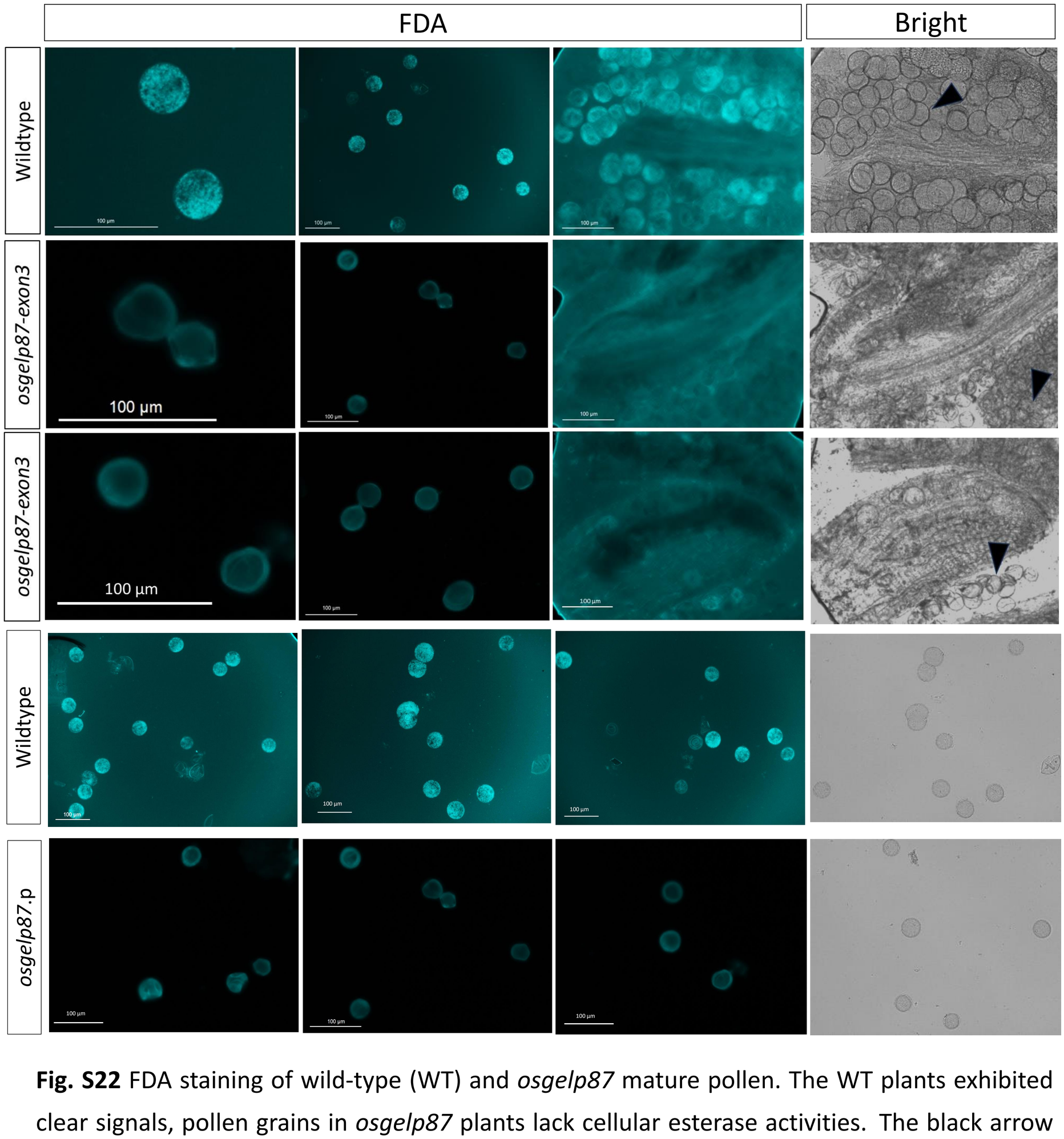

Fig. S22 FDA staining of wild-type (WT) and *osgelp87* mature pollen. The WT plants exhibited clear signals, pollen grains in *osgelp87* plants lack cellular esterase activities. The black arrow show the pollen grain aggregate.

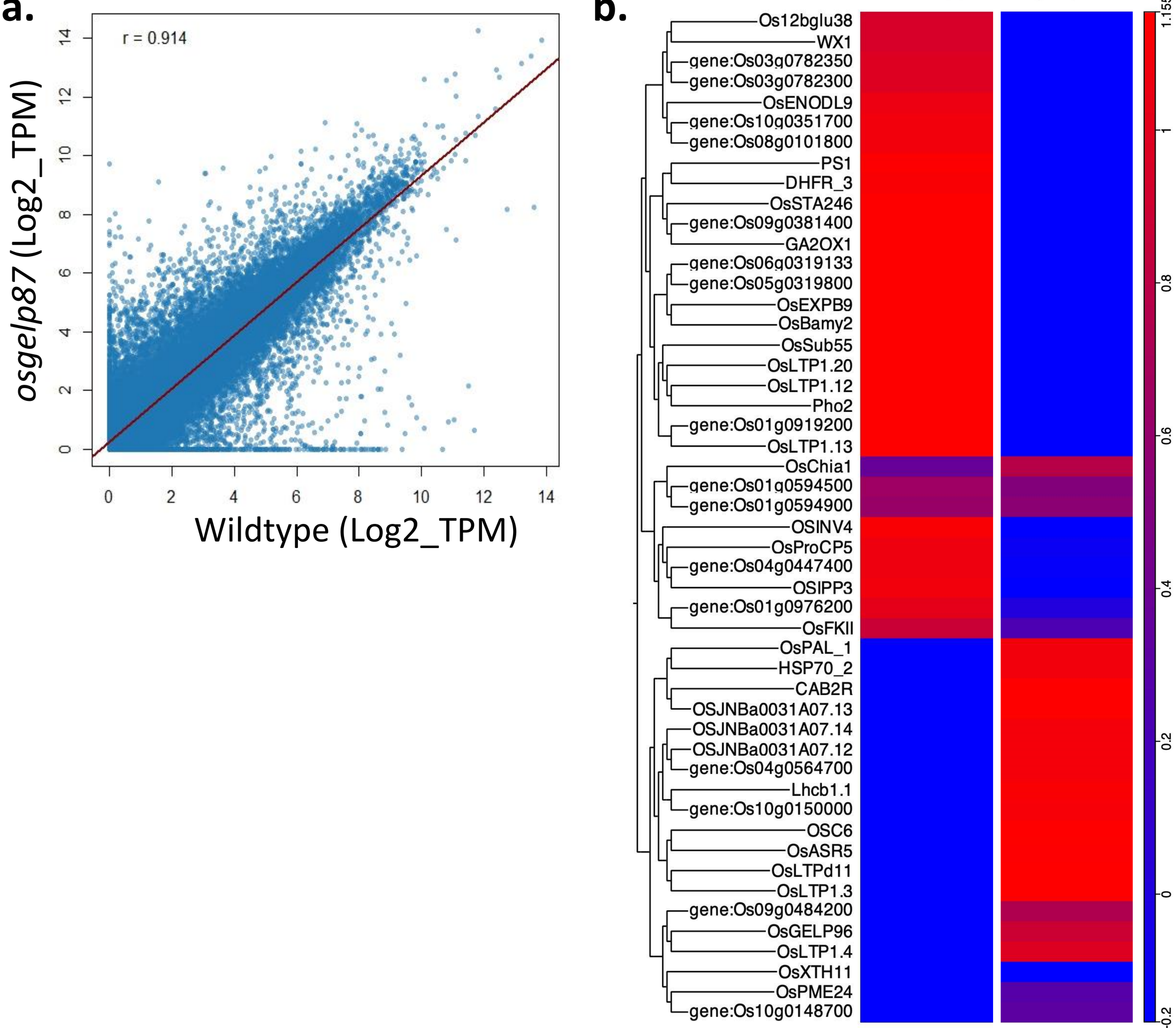

Fig. S23 Transcriptome analysis of wild-type and *osgelp87* mutant rice. (a) Scatter plot comparing gene expression levels (log_2 TPM) between wild-type and *osgelp87*. Each dot represents an individual gene. The correlation coefficient (r = 0.914) indicates a strong positive correlation between the two genotypes. **(b)** Heatmap of differentially expressed genes (DEGs) between wild-type and *osgelp87*. Genes were clustered based on expression patterns, with red representing high expression and blue representing low expression.

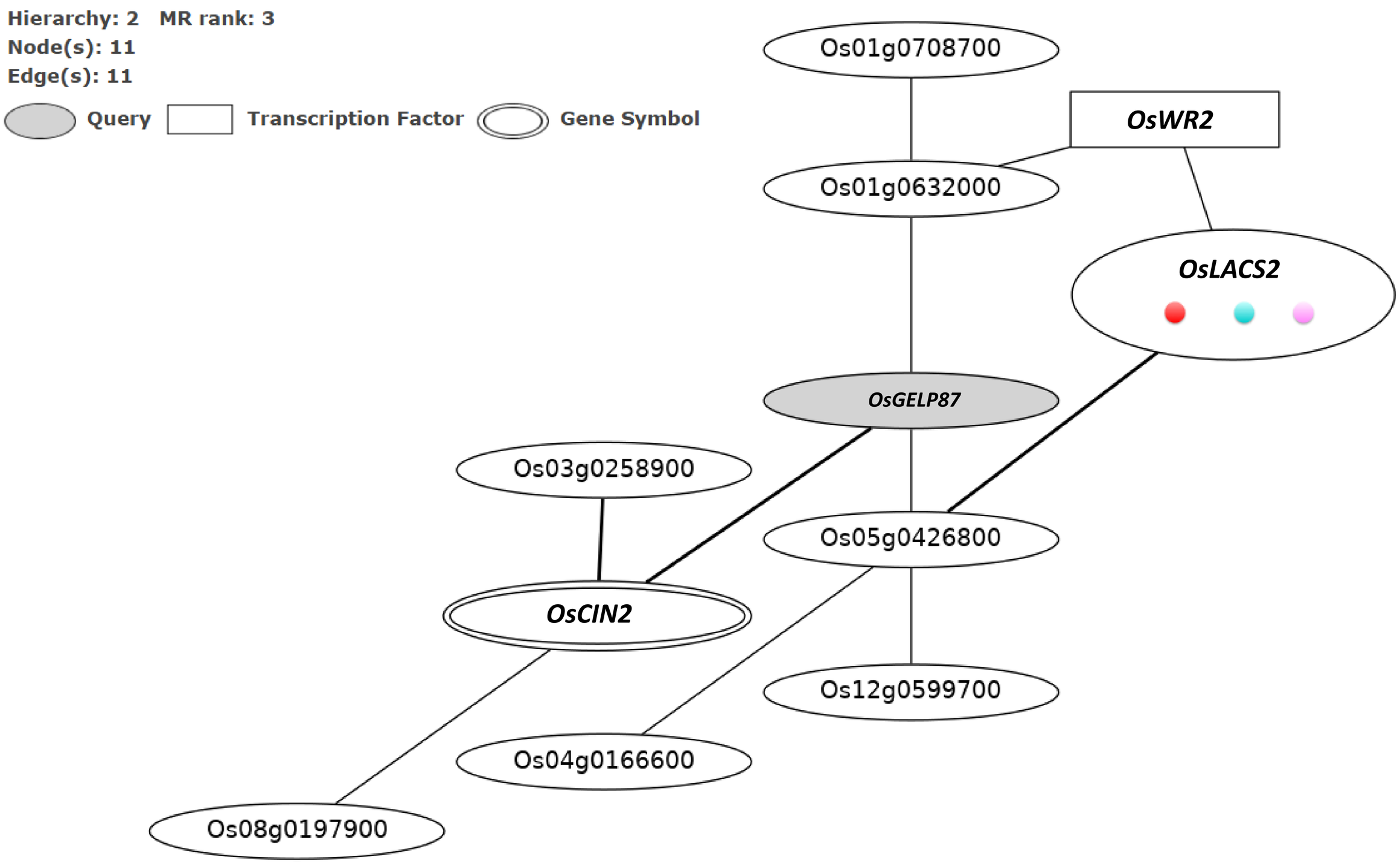

Fig. S24 *Coexpression network and KEGG pathway annotation of Os11g0558300 (OsLACS2) in rice.* Coexpression analysis using the **RiceFREND database** (https://ricefrend.dna.affrc.go.jp/) revealed a strong association between *OsLACS2* (Os11g0558300) and *OsGELP87* (Os06g0636700), together with other genes involved in lipid and carbohydrate metabolism, such as *OsCIN2* (cell wall invertase). This network suggests a coordinated lipid–sugar interaction during anther development and cold stress response. The KEGG pathway annotation (right panel) shows that *OsLACS2* participates in **metabolic pathways** (osa01100; red), **fatty acid metabolism** (osa00071; cyan), and **peroxisome** (osa04146; pink), supporting its role in fatty acid activation, lipid turnover, and peroxisomal metabolism.

Supplementary Tables

Table S1. List primers and sequences

No	Gene/plasmid name	Primer name	Sequence
1	*OsGELP87*	OsGELP87 Ter-Pro-1F	CCTCCGACATGAAGTCCGG
		OsGELP87 Ter-Pro-1R	CCCCTCGATGCAACCTTGAA
2	*Cas-9*	Cas9-F	GCTAACCTCGCTGGATCTCC
		Cas-9-R	CCTCCCCTCTCAGCCTTAGT
3	*OsGELP87*	OsGELP87-Exon3-F	TGCTCAGAACTGTTGCATGT
		OsGELP87-Exon3-R	TCATCACATTGGAACGGTGT
4	*OsGELP87*	OsGELP87-Exon2-F	TGGTTGAAGGCAGTGATCCC
		OsGELP87-Exon2-R	AAACAAAGTGCATGCGACCA
5	*OsGELP87*	OsGELP87-CAPS-F	TGGAGAACTACTTCCTCCTCGT
		OsGELP87-CAPS-R	CGTTGAGCTTGACGTTGTAGTC
6	*pMR426*	Destination-vec426 Seq	GCGCCGAGCTCATATGAAGA
7	*OsGELP87*	sgRNA_OsGELP87_Pro_F	GTTGGTGTACAGTATACAGTAGAG
		sgRNA_OsGELP87_Pro_F	AAACCTCTACTGTATACTGTACAC
8	*OsGELP87*	sgRNA_OsGELP87_Ex1_F	GTTGCACGGGGAACAATAACGTGG
		sgRNA_OsGELP87_Ex1_R	AAACCCACGTTATTGTTCCCCGTG
9	*OsGELP87*	sgRNA_OsGELP87_Ex2_F	GTTGCGCACGCTCAACGCCCTCCG
		sgRNA_OsGELP87_Ex2_R	AAACCGGAGGGCGTTGAGCGTGCG
10	*OsGELP87*	sgRNA_OsGELP87_Ex3_F	GTTGGGGGGTTCTTCTCGTTGCAG
		sgRNA_OsGELP87_Ex3_R	AAACCTGCAACGAGAAGAACCCCC
11	*OsAPX1*	OsAPX1-qRTPCR-F	CATCTCCTACGCCGATTTCTAC
		OsAPX1-qRTPCR-F	CCTTGGTAGCATCAGGAAGAC
12	*OsRboh1*	OsRboh1-qRTPCR-F	AGAACTGTTTTCTCTGAGGC
		OsRboh1-qRTPCR-F	AAGTTTTGGGAATCTTGCTT
13	*OsFAD2*	OsFAD2-qRTPCR-F	GGCTGGTGCACATCTTCGTG
		OsFAD2-qRTPCR-F	CGCTCCCGGTCGTTGTAGAT

Table S2. RNA-seq expression of some flowering genes.

Locus ID	Symbol	Reference	Note	WT	*osgelp87*	Note
Os07g0695100	*OsPRR37*	Liu et al., 2015	Pseudo-response regulator 4	86.63	138.44	up reg.
Os01g0699500	*OsMKKK70*	Mei et al., 2022	Mitogen Activated Protein Kinase Kinase Kinase 70	0.00	1.44	up reg.
Os04g0517100	*OsMYB4*	Park et al., 2010	Myb transcription factor 4	1.67	4.14	up reg.
Os06g0157500	*RFT1*	Komiya et al., 2008	Rice Flowering-locus T 1	0.00	0.00	no expression
Os07g0261200	*Ghd7*	Xue et al., 2008	Heading date 7; Encodes a CCT domain protein	0.00	0.00	no expression
Os10g0463400	*Ehd1*	Doi et al., 2004	Heading date 1; Encodes a B-type response regulator	0.00	0.00	no expression
Os01g0922800	*OsMADS51*	Kim et al., 2007	MADS box gene51	152.09	202.60	no change
Os08g0105000	*Ehd3*	Matstubara et al., 2011	Heading date 3; encoding a plant homeodomain finger-containing protein	11.34	9.95	no change
Os01g0314800	*OsLEA9*	Lou et al., 2022	Late Embryogenesis Abundant Protein 9	28.91	0.92	down reg
Os08g0174500	*DTH8*	Wei et al., 2010; Yan et al., 2011	Day to heading 8; Encodes the AP3 subunit of heme activator protein (HAP) complex	10.56	1.45	down reg